JGR Earth Surface

RESEARCH ARTICLE
10.1029/2023JF007117

Experiments on Gravel-Sand Transitions: Behavior of the Grain Size Gap Material

Elizabeth H. Dingle[1,2] **and Jeremy G. Venditti**[3]

[1]Department of Geography, Simon Fraser University, Burnaby, BC, Canada, [2]Department of Geography, Durham University, Durham, UK, [3]School of Environmental Science, Simon Fraser University, Burnaby, BC, Canada

Key Points:

- Gravel beds composed of 2–8 mm particles cannot maintain a stable slope when sand is added to the bed material
- Stable gravel-sand transitions cannot be produced by washload deposition where gravel beds are composed of 2–8 mm particles
- Enhanced relative mobility of grain size gap particles occurs when medium sand falls out of washload at the gravel-sand transition

Correspondence to:
E. H. Dingle,
elizabeth.dingle@durham.ac.uk

Citation:
Dingle, E. H., & Venditti, J. G. (2023). Experiments on gravel-sand transitions: Behavior of the grain size gap material. *Journal of Geophysical Research: Earth Surface*, *128*, e2023JF007117. https://doi.org/10.1029/2023JF007117

Received 17 FEB 2023
Accepted 9 NOV 2023

Author Contributions:
Conceptualization: Elizabeth H. Dingle, Jeremy G. Venditti
Data curation: Elizabeth H. Dingle
Formal analysis: Elizabeth H. Dingle
Funding acquisition: Jeremy G. Venditti
Methodology: Elizabeth H. Dingle, Jeremy G. Venditti
Supervision: Jeremy G. Venditti
Visualization: Elizabeth H. Dingle
Writing – original draft: Elizabeth H. Dingle
Writing – review & editing: Elizabeth H. Dingle, Jeremy G. Venditti

Abstract River bed sediments often lack fine gravel between 1 and 5 mm, a phenomenon referred to as the "grain size gap." The gap corresponds to the rapid reduction in grain size associated with the gravel-sand transition (GST), where median bed material grain size reduces from ~10 mm gravel to ~1 mm sand. Fine gravel grain sizes are often present in hillslope sediment, so it is not clear why they are absent on riverbed surfaces. We present a phenomenological laboratory experiment examining changes in sediment dynamics across a GST to examine the behavior of grain size gap material when included in the bed and feed grain size distributions. Our observations indicate that where sand falls out of washload, forming persistent surficial deposits at the GST, grain size gap material experiences enhanced mobility. This is due to hydraulic smoothing by sand that occurs because of a geometric effect, where medium sand bridges interstitial pockets in fine gravel bed surfaces. Our experiments show that gap gravel flux is enhanced by sand deposition, making gravel beds mobile at the threshold of motion. We are unable to maintain an immobile grain size gap gravel bed when sand is fed which explains why gravel beds composed of 1–5 mm particles are so rare on Earth. We hypothesize that in natural systems, grain size gap particles are either buried in the diffuse extension of GSTs or transported into coastal and marine environments where they are more commonly observed.

Plain Language Summary There are very few river beds made up of 1–5 mm gravel particles. That is not to say that these grain sizes do not exist, but that they rarely form the dominant grain size in river beds. This grain size gap is most obvious where river beds rapidly transition from gravel (~10 mm) to sand (~1 mm) at the gravel-sand transition. We undertook a flume experiment looking at the behavior of grain size gap particles at gravel-sand transitions. We tried to build a gravel-sand transition with 2–8 mm particles in the gravel bed, but when we fed sand onto the gravel bed, the previous static bed started moving and was transported out of the flume. We also tried to mix grain size gap particles into a coarser gravel bed and found that gap particles became disproportionately mobile when sand settled on the bed. Our experiment suggests that gap particles are transported across the transition where they may then be buried in the sand reach. As such, stable gravel beds of this grain size are rarely observed on Earth.

1. Introduction

River bed sediments gradually fine downstream in the absence of lateral inputs, until median grain sizes reduce to 5–10 mm (Paola et al., 1992; Rice, 1999; Sambrook Smith & Ferguson, 1995; Sternberg, 1875; Yatsu, 1955). At this point, there is then an abrupt reduction in grain size to sand that can occur over a distance as little as a few channel widths, called the gravel-sand transition (GST) (Dingle et al., 2017, 2021; Ferguson et al., 1996, 2011; Frings, 2011; Kodama, 1994; Sambrook Smith & Ferguson, 1995; Shaw & Kellerhals, 1982; Venditti & Church, 2014; Yatsu, 1955). The GST is marked by a change from a framework-supported gravel to a matrix-supported sand bed structure (Frings, 2011; Venditti & Church, 2014). A related phenomenon is a gap in riverbed sediment size distributions between ~1 and 5 mm (Carling & Reader, 1982; Shaw & Kellerhals, 1982; Trampush et al., 2014; Udden, 1914). The bounds of the grain size gap may vary, but the phenomenon are so ubiquitous that there is a paucity of river beds with median bed grain sizes of ~1–5 mm on Earth (e.g., Dingle et al., 2021; Lamb & Venditti, 2016). The GST, grain size gap and absence of fine gravel bed rivers are interrelated. Experiments with bimodal sediments can produce GSTs (e.g., Gran et al., 2006; Paola et al., 1992; Sambrook Smith & Ferguson, 1995; Wilcock, 1998; Wilcock et al., 2001) and numerical models of downstream fining where bimodal or binary grain size distributions are imposed produce a sharp grain size transition from fine gravel to sand (An et al., 2020; Blom et al., 2017; Cui & Parker, 1998; Ferguson, 2003; Hoey & Ferguson, 1994;

Parker & Cui, 1998). Sharp transitions from medium gravel to sand leave little room for rivers with a fine gravel bed in the downstream fining profile.

There are several proposed reasons for the grain size gap including (a) viscous damping of particle collisions limiting the production of fine gravel sizes (Jerolmack & Brzinski, 2010), (b) preferential abrasion of fine gravel grain sizes (Kodama, 1994; Shaw & Kellerhals, 1982; Yatsu, 1955), (c) an absence of fine gravel production at weathering sites (Wolcott, 1988), (d) transport mode separation where fine gravel is present but split between gravel and sand bed reaches of a river (Lamb & Venditti, 2016; Venditti & Church, 2014; Venditti et al., 2015), and (e) hydraulic sorting of gravel where gap sizes are preferentially entrained in bedload (Church & Hassan, 2023). Viscous damping is not a likely cause of the gap because experiments have shown that collisions are not damped in the gap sizes (Scheingross et al., 2014). While preferential abrasion of gap sediments may occur in mechanically weaker lithologies (e.g., Kodama, 1994), gap material is common in energetic shallow marine environments (e.g., Jennings & Shulmeister, 2002; McLean, 1970) and in gravel bed subsurface deposits (e.g., Ferguson et al., 1989; Gomez et al., 2001; Mason et al., 2019), suggesting that preferential abrasion of fine gravel is not a universal cause of the grain size gap. Similarly, source limitations may locally explain grain size gaps (e.g., Wolcott, 1988), but gap material is often present on hillslopes (Sklar et al., 2017, 2020), suggesting this is not a universal cause.

There is more supporting evidence for grain size gap development through hydraulic sorting and transport mode separation. Early documentation of the grain size gap suggested that it occurred because of the preferential entrainment and transport of fine gravel (Russell, 1968; Sundborg, 1956; Udden, 1914), but no specific mechanism was invoked by these earlier works. Depletion of fine gravel is a common observation in experiments of gravel bed transport (e.g., Elgueta-Astaburuaga & Hassan, 2017, 2019; Elgueta-Astaburuaga et al., 2018; Hassan et al., 2020). Church and Hassan (2023) experimentally show that 1–8 mm grains tend to outrun both larger and smaller grains in a sediment mixture on a gravel bed, enhancing bimodality because the bed becomes enriched in relatively immobile >8 mm grains, while sand infiltrates the bed, and fine gravel runs out of the experimental flume.

Size selective transport in gravel-sand mixtures is a well-documented phenomenon where increasing sand content increases the gravel transport rate until the sand content is so great it buries the gravel (An et al., 2019; Curran & Wilcock, 2005; Hill et al., 2017; Ikeda & Iseya, 1988; Jackson & Beschta, 1984; Venditti et al., 2010a, 2010b; Wilcock, 1998; Wilcock & Kenworthy, 2002; Wilcock & McArdell, 1993, 1997; Wilcock et al., 2001). Gravel transport is enhanced by the addition of finer sediment due to a hydraulic smoothing effect where finer particles fill the pockets between the coarser gravel, increasing near bed velocity and reducing the flow resistance of the bed (Venditti et al., 2010a, 2010b). This enhances the mobility of coarse particles as the velocity differential around protruding particles causes larger drag forces on those particles (Venditti et al., 2010a). The smoothing effect can only be effective where the pockets of the gravel are filled with finer sediment.

The propensity of finer sediment to infill pockets in a gravel surface is dependent on a grain size ratio calculated as

$$D_* = \frac{D_{50c}}{D_{50f}} \tag{1}$$

where D_{50c} and D_{50f} are the median sizes of the coarser bed and finer sediment feed, respectively (Hill et al., 2017). At $D_* > 20$, fine sediment percolates through a gravel framework while at $D_* < 2$ a gravel bed will aggrade, but without mobilizing the coarser fraction (Hill et al., 2017). When $2 < D_* < 20$, the fine sediment fills pockets on the gravel matrix due to bridging of grains in the pores of the gravel, enhancing the mobility of coarser sediment (Dudill et al., 2020; Hill et al., 2017). Bridging occurs when fine sediment jams between grains blocking deeper infiltration and occurs when the feed is fine enough to infiltrate into the upper layer of a static bed (a depth equivalent to 2.5–5 times the largest particles) but too coarse to percolate freely into the subsurface (Dudill et al., 2017, 2020; Gibson et al., 2010). Whether this geometric argument extents to grain size fractions and ratios beyond gravel and sand (e.g., gravel feed onto a cobble bed) is unknown, but the absence of abrupt grain size transitions between other grain size fractions would suggest this is not purely a geometric effect (e.g., Parker et al., 2023).

Transport mode separation may also cause the grain size gap. Lamb and Venditti (2016) argued theoretically that the grain size gap can emerge due to Reynolds number effects on the bedload and suspension entrainment thresholds which prevent the formation of riverbeds composed of 1–5 mm particles. They showed that the shape

of bedload and suspension threshold curves indicate that when the 90th percentile of a grain size distribution (D_{90}) disperses from the bedload, the finest particles (D_{10}) in suspension transition from washload to suspended bed material load, forming persistent sand deposits on the bed. The shape of the bedload and suspension threshold curves leads to a dramatic change in the behavior of the median size (D_{50}) at a formative shear velocity $u*_f = 0.1$ m/s and a restricted range of hydraulic conditions under which gravel beds composed of 1–5 mm can exist. When $u*_f > 0.1$ m/s, gravel bed conditions exist because gravel is transported as bedload and sand is transported as washload, without persistent deposits on the bed. When $u*_f < 0.1$ m, fine gravel disperses and persistent deposits of sand develop, forming a sand bed. Lamb and Venditti (2016) argued that this effect could produce a bimodal grain size distribution because the effect could split the supplied gap material between gravel and sand bed deposits so that it appears to be depleted.

GST is an excellent place to explore the grain size gap because it is the location in the fluvial system where the gap is best expressed and where the presence of the gap has morphological consequences (e.g., Dingle et al., 2020). The presence of the gap causes GSTs in bedload dominated systems (Ferguson, 2003; Ferguson et al., 1996; Paola et al., 1992; Wilcock, 1998) and sharpens the grain size reduction across the transition (Lamb & Venditti, 2016). In a companion paper, we used a phenomenological flume experiment to examine sediment dynamics across the GST, specifically focusing on changes in sand transport across the GST (Dingle & Venditti, 2023). We formed a gravel wedge where particles were at the threshold of motion, then fed sand onto the gravel wedge and found that sand is carried as washload when gravel is at the threshold of motion. At the terminus of the gravel wedge, there is a change in suspension dynamics where the washload transitions to the bed material load at $u*_f$ of ∼0.1 m/s. In this initial experiment, particles in the grain size gap range were not present in the initial bed or sediment feed grain size distributions. Here, we undertake a further experiment to specifically explore the behavior of grain size gap material at GSTs. The objective of our experiment is to (a) examine how gap gravel behaves in the gravel bed and sediment feed at the GST, (b) explore how sand deposition from washload influences selective entrainment of gap gravel, and (c) determine the morphological consequences of washload deposition and gap gravel behavior at the GST.

2. Methods

2.1. Experimental Design

Grain size gap material was introduced into the experiments in three ways. The first six runs of our experiment (Runs 9–14) were designed to examine how a stable GST responds to variations in the size of supplied sediment. We separately added a fine grain size gap (FGG; 2.5–5.6 mm) feed and a coarse grain size gap (CGG; 5.6–8 mm) feed onto a stable GST composed of non-grain size gap (NGG; 8–16 mm) gravel, and then repeated the runs with differing quantities of gap-sized material mixed into the bed. The final two runs (Runs 15–16) were designed to examine the effects of a sand feed on different bed distributions of clean gravel containing various quantities of FGG and CGG (with no initial sand content).

Following Dingle and Venditti (2023) we elected to study gravel exhaustion GSTs in Runs 9–14 where we built a stable GST that was temporally and spatially fixed, with gravel at the threshold for entrainment and a constant sand feed. The justification for this is based on observations from gravel bed rivers where gravel is transported only a few days or weeks per year, during which sand is carried as washload without forming persistent deposits on the bed and gravel is at the threshold of motion (e.g., McLean, 1990; Reid et al., 2007). During the rest of the year, gravel mobility is limited in many natural gravel bed rivers, but sand is transported continuously (e.g., Church et al., 1991; Kuhnle, 1993; Wathen et al., 1995; Wilcock, 1998).

Global analysis of GSTs has established that the only universal morphological characteristic is an abrupt reduction in grain size from fine gravel (often 5–10 mm) to sand grain sizes (Dingle et al., 2021). As such, in Runs 9–14, we focused on forming a gravel wedge characterized by ∼5–10 mm grain sizes that was at the threshold of motion; then, we fed sand to mimic the deposition of sand from washload and create a stable GST in the flume. We then turned on a grain size gap feed to examine how these grain sizes interact with the gravel reach and the stability of the GST. Runs 15 and 16 were designed to examine the behavior of grain size gap gravel mixed into a wider gravel bed distribution with a sand feed. In these runs, the initial bed was entirely gravel with no GST in the flume.

Our experiments are phenomenological and not designed to replicate or serve as a scaled model of a natural river channel, but instead to study granular dynamics that occur at GSTs. We selected a relatively short flume (5 m) because it allowed us to isolate the suspension deposition mechanism without the complications of downstream fining and profile concavity that are widely thought to occur due to selective transport, particle

abrasion, and in situ weathering. We selected a narrow flume width (34 mm) to eliminate cross-stream transport, lateral sorting, 3D bedform and bar formation, but wide enough to avoid particle jamming (Church & Zimmermann, 2007). The narrow flume also allows direct observation of all grains in motion in the channel, which is an important component of our study. The use of narrow flume experiments is an established approach to explore granular dynamics that may be applied to our understanding of sediment transport in fluvial systems (e.g., Ancey & Pascal, 2020; Benavides et al., 2022, 2023; Deal et al., 2023; Dudill et al., 2017, 2020; Frey et al., 2020; Pascal et al., 2021). Our experiment takes advantage of the "unreasonable effectiveness" approach to geomorphology experimentation (Paola et al., 2009) and we only scale parameters that we expect control the processes of interest. In doing so, we are testing whether a particular set of variables is capable of producing a phenomenon.

Care must be taken in extrapolating from unscaled phenomenological experiments to natural systems (Paola et al., 2009). Nevertheless, we designed the experiments so that the grain size ratios match those found in natural channels at the GST, and were able to maintain transport stages that are also comparable to natural channels. That suggests that our experiments are able to replicate the granular dynamics of interest, even though direct extrapolation to fluvial systems is not possible.

Our experimental flume tends to produce trans- and super-critical flows at shear stresses large enough to produce gravel transport. Particle dynamics are controlled by lift and drag forces that are set by the distribution of fluid velocities of a particle. The drag (F_D) and lift (F_L) forces on a submerged particle are calculated as

$$F_D = 0.5\rho\langle u\rangle^2 C_D A \tag{2}$$

$$F_L = 0.5\rho\langle u\rangle^2 C_L A \tag{3}$$

where ρ is the density of water, u is the local velocity and the angle brackets denote a spatial average over A, the upstream facing surface area of the particle exposed to the flow, C_D is a drag coefficient, and C_L is the lift coefficient that must be estimated empirically (Lamb et al., 2008, 2017; Schmeeckle et al., 2007; Wiberg & Smith, 1987). Neither Equations 2 or 3 have a dependence on the Froude number, but Flammer et al. (1970) showed that dra significantly increases with shallows due to particle surface wave effects, so one could argue that the presence of surface waves could impact the drag and lift forces that affect sediment entrainment and transport, but only in very shallow flows ($h/D < 1$). Lamb et al. (2017) explored how C_D and C_L are affected by relative submergence by directly measuring C_D and C_L in shallow flows and found that when the particles are not fully submerged, the C_L is affected by surface waves. However, when fully submerged ($h/D > 2$), the drag and lift coefficients showed little variability with the Froude number (Lamb et al., 2017). The relative submergence with trans-critical and super-critical flows in our experiment is between 2 and 5, so it is reasonable to surmise that the Froude number in our experiment had no impact on particle lift and drag force distributions.

2.2. Experimental Setup and Procedure

The experiment was conducted in a 5 m long and 34 mm-wide flume (Dingle & Venditti, 2023). Water was recirculated but sediment was not. A 50 mm high block inserted at the end of the flume prevented bed sediment from washing out. Flow spilled over the block at the end of the flume with no upstream effects. In all experiments, a gravel bed was placed in the flume, then separate sand and in some instances gravel feeds were introduced at constant rates using two sediment hoppers at the top end of the flume. The composition of the initial bed and sediment feed was varied systematically to examine the behavior of the gap material (Table 1).

In Runs 9–12, a stable GST was developed using the same experimental procedure outlined in Dingle and Venditti (2023) (Table 1). The composition of the initial bed material was a narrow distribution of NGG (D_{50} = 9.8 mm) in Runs 9 and 10, and a broader distribution of 5.6–16 mm (D_{50} = 8.2 mm) gravel in Runs 11 and 12 (Figure 1) that contained 46% CGG. Gravel was deposited at the top end of the flume and reworked by an imposed water discharge so that the gravel mixture was at the threshold of motion. Once the wedge stabilized, a 0.57 mm sand feed was turned on (Figure 1). Sand was transported as washload through the gravel reach and then started to deposit in the lower half of the flume, forming a sand reach. Once this stable condition was established, a separate gravel feed was turned on in addition to the sand feed in Runs 9–12 (Table 1). We considered runs to be complete when either the GST prograded to the end of the flume and the position of the GST had remained stationary for ~5 min (Runs 9–12).

Table 1
Run Numbering and Perturbation Description

Run ID	Run description	Run type	Initial gravel bed material	Composition of feed(s)
Run 9	Gap material in the feed only (stable GST)	Addition of a FGG[a] feed to a stable NGG[b] transition	NGG (8–16 mm) + 0.57 mm sand	0.57 mm sand + 2.8–5.6 mm gravel (FGG)
Run 10	Gap material in the feed only (stable GST)	Addition of a CGC[c] feed to a stable NGG transition	NGG (8–16 mm) + 0.57 mm sand	0.57 mm sand + 5.6–8 mm gravel (CGG)
Run 11	Gap material in the feed and bed (stable GST)	Addition of a FGG feed to a stable mixed gap/non-gap gravel transition	5.6–16 mm (54% 8%–16% and 46% 5.6–8 mm) + 0.57 mm sand	0.57 mm sand + 2.8–5.6 mm gravel (FGG)
Run 12	Gap material in the feed and bed (stable GST)	Addition of a CGG feed to a stable mixed gap/non-gap gravel transition	5.6–16 mm (54% 8%–16% and 46% 5.6–8 mm) + 0.57 mm sand	0.57 mm sand + 5.6–8 mm gravel (CGG)
Run 13	Gap material in the bed (no GST)	CGG bed with sand feed	CGG (5.6–8 mm)	0.57 mm sand
Run 14	Gap material in the bed (no GST)	FGG bed with sand feed	FGG (2.8–5.6 mm)	0.57 mm sand
Run 15	Gap material in the bed (no GST)	Narrow distribution gravel (with CGG) with sand feed	Unimodal gravel (4–16 mm)	0.57 mm sand
Run 16	Gap material in the bed (no GST)	Wide distribution gravel (with FGG + CGG) with sand feed	Unimodal Gravel (2–22 mm)	0.57 mm sand

[a]Fine Gap Gravel (FGG) refers to 2.8–5.6 mm particles. [b]Non-Gap Gravel (NGG) refers to 8–16 mm particles. [c]Coarse Gap Gravel (CGG) refers to 5.6–8 mm particles.

In Runs 13–16, the flume was initially filled entirely with gravel (i.e., there was no GST or sand in the bed; Table 1) with grain size distributions that varied from narrow distributions of gap material to wider distributions that included coarser particles as well (Figure 1). Water was turned on and the gravel bed adjusted to a near

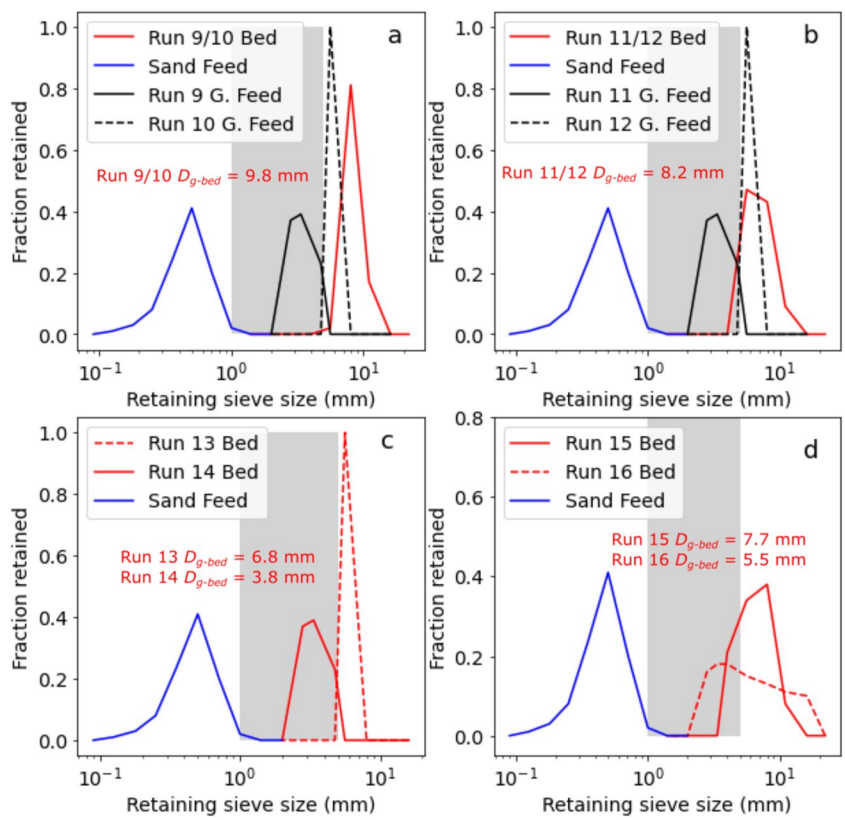

Figure 1. Grain size distributions of the initial bed and sediment feeds used in all runs. The gravel mode median ($D_{g\text{-bed}}$) is noted for each initial bed. The gray box denotes the grain size gap (1–5 mm) range. (a) Runs 9 and 10 with gap material in the feed, (b) Runs 11 and 12 with gap material in the feed and bed, (c) Runs 13 and 14 with gap material in the bed, (d) Runs 15 and 16 with gap material in wider gravel distributions.

threshold condition where the bed was visually immobile, having adopted a constant slope with individual grains not moving. Then, a 0.57 mm sand feed was turned on. We considered runs to be complete when a new slope was established where gravel particles were immobile. This was also retrospectively confirmed by measuring the sediment output from the flume where final sand outputs were within 5% of the sand feed rate.

2.3. Observations and Calculations

We measured the position of the GST, which was a 0.2–0.4 m region of patchy gravel and sand, similar to the diffuse extension observed in many GSTs (cf. Venditti & Church, 2014; Venditti et al., 2015). We recorded the position of the GST where the first persistent patches of sand covering gravel were observed on the bed. It was not possible to quantify separate fluxes for washload and suspended bed material load without fundamentally altering the phenomena we sought to examine; therefore, we made direct visual observations of the transport mode over several minutes to compare against nominal thresholds of suspension retrospectively calculated from reach-averaged flow conditions. Washload occurs when there is suspended sediment transport but no persistent deposition on the bed surface (Bagnold, 1966; Church, 2006; Einstein, 1950), although washload does interact with the bed and can fill interstitial pores in gravel (Einstein, 1968; Lamb et al., 2020). Suspended bed material transport occurs when suspended sediment forms persistent deposits on the bed that become a source of the material in suspension (Church, 2006; Garcia, 2008; Lamb et al., 2020).

Initial unperturbed bed surface grain sizes were determined from the distributions of the input gravel mixtures, and an assumed 15% sand cover in Runs 9–12. This coverage was assumed rather than directly measured as it was difficult to accurately distinguish the relatively small fraction of sand on the bed from gravel particles through flowing water and the sand coverage was not characteristic of the bed with the flow off. This is a typical value for the volumetric content of sand in clean gravel bed rivers where sand only fills interstitial spaces (e.g., McLean, 1990; Shaw & Kellerhals, 1982), although this may overestimate sand coverage where surface distributions are typically less than volumetric content (e.g., Graham et al., 2005). Bed surface grain size measurements were made during each run and at the end (with the water supply turned off) using overhead photos where possible. The initial unimodal gravel bed in Runs 9 and 10 was painted yellow, while grain sizes within the grain size gap fractions were black to allow final bed grain size statistics to be calculated easily. To do this, the coverage of each grain size fraction was digitized manually from 2 to 3 digital images in the gravel reach. Owing to the small-scale nature of our experiment, most of the gravel reach was captured within 2–3 overhead photos, where care was taken to exclude regions of enhanced sand deposition at the GST and its diffuse extension. Final grain size distributions were calculated by scaling the grain size distributions of each fraction based on its percentage surface coverage. In Runs 15 and 16, gravel grain size fractions were painted in separate colors at 0.5-phi unit intervals. In Runs 11, 15, and 16 it was not possible to accurately differentiate separate grain size fractions from photos of the final bed because the FGG and CGG grains were the same color (Run 11) or colors were too similar between fractions to confidently identify (Runs 15 and 16). In Run 11, we assumed that the bed was 50% FGG and 50% CGG gravel based, which is consistent with the examination of images. For Runs 15 and 16, we only report % sand cover of the final bed. After the perturbation caused by the sediment feed in Runs 10, 11, 13, 14, 15, and 16 (Table 1), sediment exiting the flume was trapped, dried, sieved and weighed by grain size fraction.

In each run we measured discharge after the GST was formed (Runs 9–12) or the gravel bed stabilized (Runs 13–16), but before the additional gravel or sand feed began. Measurements of flow depth (h) and water surface gradient (S) were made for each initial condition, and at the end of the run. Reported h is reach averaged, based on many measurements made in each gravel and sand reach (Runs 9–12). In Runs 13–16, where no GST was present, three or four flow depth measurements were taken along the length of the flume and averaged. Individual depth measurements varied by <8% in all instances. Gradient was calculated as a reach average for the gravel and sand reaches based on relative bed elevations measured at the same location as the flow depth measurements. The bed elevation was defined as a line through the centroid of the surface gravel particles. We calculated the reach-averaged velocity as $\overline{U} = Q/(hw)$ where Q is water discharge and w is flume width. The particle Reynolds number (R_p) was calculated for both the gravel and sand reach in each run:

$$R_p = \frac{D_{50}\sqrt{RgD_{50}}}{\upsilon} \tag{4}$$

where v is the kinematic viscosity of water, and R is submerged specific gravity incorporating the density of water (ρ) and sediment (ρ_s) where $R = \rho_s/\rho - 1$ (Garcia, 2008). Reach-averaged shear velocity (u_r^*) for both the gravel and sand reaches was also calculated from a reach-averaged shear stress (τ) where:

$$u_r^* = \sqrt{\frac{\tau}{\rho}} = \sqrt{ghS} \tag{5}$$

where g is the acceleration due to gravity and S is the water surface slope. In a narrow flume, a substantial portion of the total force is applied to the sidewalls and therefore not available to transport sediment, so we applied the Williams (1970) sidewall correction. Local shear velocity estimates made from double-averaged velocity profiles measured with a laser Doppler anemometer were similar to side wall corrected u_r^* in the gravel reach, but u_r^* in the sand reach was consistently less (by 40%–50%) (see Dingle & Venditti, 2023). Both the velocity profiles and u_r^* values showed a substantial reduction in shear stress across the transition.

To characterize gravel mobility, the Shields number was calculated from

$$\tau^* = \frac{\tau}{(\rho_s - \rho)gD_{50}} \tag{6}$$

where $\tau = \rho u_r^{*2}$. Values of $\tau_* < 0.045$ are widely accepted as characterizing conditions below the entrainment threshold for a gravel mixture (Miller et al., 1977; Yalin & Karahan, 1979), but this value can vary depending on the gravel size distribution and sand content (e.g., Wilcock & Crowe, 2003) and bed surface structure which can increase the entrainment threshold τ_* to as high as 0.117 (Church & Hassan, 2005; Church et al., 1998; Hassan et al., 2020). To account for the gradient of the gravel reaches established in the flume, we also calculated a slope-corrected incipient Shields number (Lamb et al., 2008) to compare our observed values against

$$\tau_c^* = 0.15S^{0.25} \tag{7}$$

Particle settling velocities (ω) were calculated using the Ferguson and Church (2004) method to calculate a suspension ratio (u_r^*/ω). Incipient bed material suspension occurs when $u_r^*/\omega > 0.4$ when the flow is hydraulically rough ($R_p > 27.5$) and is a function of R_p when $R_p < 27.5$ (Niño et al., 1994, 2003). The transition to washload is typically assumed to occur at three times the suspension threshold ($u_r^*/\omega = 1.2$) although this boundary is not exact (Bridge, 2009). The advection length (A_L) for sand being fed into the flume was also calculated as

$$A_L = \overline{U}h/\omega. \tag{8}$$

Venditti et al. (2015) showed that when $A_L \approx$ channel width, suspended bed material transport occurs, but when $A_L >>$ channel width, washload transport dominates.

3. Results

3.1. Establishing Stable GSTs in Runs 9–12

Adding a sand feed to the gravel wedge to develop the stable GST in Runs 9–12 led to sand being exchanged with the bed without forming persistent deposits, which is consistent with a washload condition (Einstein, 1968). The advection length for sand was >> channel width in our initial or equilibrium conditions (Table 2), also consistent with washload conditions (Venditti et al., 2015) and our own visual observations. Perhaps more importantly, the advection length is << than the reach gravel reach length, indicating that sand could have deposited in the reach, but did not. When the sand feed was initially turned on, sand filled the gravel matrix when it momentarily exchanged with the bed surface, gradually filling the gravel subsurface matrix. Once the matrix was full, the sand feed bypassed the gravel reach and deposited near the toe of the gravel wedge, forming a sand reach in the lower half of the flume. In all runs, flow was hydraulically rough in the gravel reach (i.e., $R_p > 27.5$; Niño et al., 2003) indicating a suspension threshold of $u_r^*/\omega > 0.4$ and washload threshold of $u_r^*/\omega > 1.2$ for the sand (Table 2).

The τ^* value of the initially stable gravel wedge in Runs 9–12 was greater than the widely accepted nominal threshold of motion for gravel mixtures of 0.045 (Table 2) (e.g., Miller et al., 1977; Yalin & Karahan, 1979), but is consistent with the slope-dependent values (Lamb et al., 2008). Measured τ^* values are generally comparable or slightly lower than these slope-dependent threshold values. The relatively narrow breadth of the bed grain size

Journal of Geophysical Research: Earth Surface

10.1029/2023JF007117

Table 2
Initial and Final Conditions for Runs 9–16 in Gravel (g) and Sand (s) Reaches of the Flume

Run ID	Q (l/s)	S (initial/final)	h (cm) (initial/final)	$\overline{U}$ (m/s)	u_r^* (m/s) (initial/final)	Bed gravel mode D_{50} (mm) (initial/final)	Re_p (initial/final)	u_r^*/ω (initial/final)	A_L (m)	Gravel reach τ^* (initial/final)	Gravel reach slope-dependent τ^*_c (initial/final)	Froude number (initial/final)	Sediment feed (D_{50} and feed rate)
9	0.532	0.115/0.043 (g)	2.75/2.85 (g)	0.57 (g)	0.12/0.07 (g)	9.8/5.1	2,074/523 (g)	1.49/0.92 (g)	0.20	0.087/0.084	0.083/0.068	1.1/1.0 (g)	Sand - 0.57 mm (3.95 g/s)
		0.022 (s)	2.70 (s)	0.58 (s)	0.05 (s)		30 (s)	0.65 (s)				1.1/1.1 (s)	FGG Gravel—3.8 mm (1.00 g/s)
10	0.546	0.084/0.048 (g)	2.75/2.80 (g)	0.58 (g)	0.10/0.08 (g)0.05 (s)	9.8/8.8	2,074/1,207 (g)	1.27/0.70 (g)	0.21	0.064/0.053	0.076/0.070	1.1/1.1 (g)	Sand - 0.57 mm (3.8 g/s)
		0.024 (s)	2.80 (s)	0.58 (s)			30 (s)	0.68 (s)				1.1/1.1 (s)	CGG Gravel—6.8 mm (0.97 g/s)
11	0.480	0.070/0.032 (g)	2.90/2.85 (g)	0.49 (g)	0.09/0.06 (g)	8.2/7.1	1,526/856 (g)	1.17/0.80 (g)	0.18	0.067/0.046	0.072/0.063	0.9/0.9 (g)	Sand - 0.57 mm (3.8 g/s)
		0.020 (s)	2.60 (s)	0.54 (s)	0.05 (s)		30 (s)	0.62 (s)				1.1/0.9 (s)	FGG Gravel—3.8 mm (1.00 g/s)
12	0.550	0.062/0.039 (g)	2.60/2.45 (g)	0.56 (g)	0.08/0.07 (g)0.05 (s)	8.2/7.1	1,526/1,169 (g)	1.08/0.84 (g)	0.19	0.056/0.041	0.070/0.067	1.1/1.2 (g)	Sand - 0.57 mm (3.8 g/s)
		0.021 (s)	2.35 (s)	0.62 (s)			30 (s)	0.62 (s)				1.3/1.2 (s)	CGG Gravel—6.8 mm (0.97 g/s)
13[a]	0.517	0.047/0.024	2.50/2.40	0.61	0.07/0.05	7.6/7.6	1,089/30	0.91/0.64	0.19	0.048/-	0.065	1.2/1.3	Sand - 0.57 mm (3.95 g/s)
14[a]	0.467	0.040/0.019	2.40/2.45	0.57	0.07/0.05	3.8/3.8	530/33	0.85/0.59	0.18	0.071/-	0.062	1.2/1.3	Sand - 0.57 mm (3.95 g/s)
15[a]	0.752	0.046/0.037	3.15/3.15	0.70	0.08/0.07	7.7/[b]	1,308/834	0.94/0.84	0.28	0.045/0.050	0.064/0.066	1.3/1.3	Sand - 0.57 mm (3.95 g/s)
16[c]	0.624	0.077/0.080 (g)	3.40/3.55 (g)	0.54 (g)	0.10 (g)	5.5/[b]	783/438 (g)	1.23/1.26 (g)	0.23	0.110/0.170	0.074/0.080	0.9/0.9 (g)	Sand—0.57 mm (3.95 g/s)
		-/0.038 (s)	-/3.60 (s)	0.51 (s)	0.07 (s)		30 (s)	0.87 (s)				0.9/0.9 (s)	

Note. Initial and final condition values are separated by "/" where relevant.

[a]In these runs, the flume was entirely gravel so there are no sand reach measurements. [b]The final gravel mode could not be directly measured. [c]A weakly defined GST developed in this run once the sand feed was turned on. Metrics are given for the gravel reach unless stated otherwise.

distributions seem to correlate with the deviation from the threshold with broader distributions having a lower threshold for motion (Table 2) (Parker, 2008). Flows were transcritical based on the Froude number in both the gravel and sand bed reaches (Table 2). The mean flow depth in our experiment was 2–3 times greater than the largest grains (Table 2).

Even with similar discharge and sediment feed conditions, our initial conditions for a formed GST vary somewhat. The most extreme example is Runs 9 and 10, which have only a few percent variation in discharge and similar bed grain sizes, but the initial slopes are substantially different (~30%). This variation is similar to that in Dingle and Venditti (2023), where the initial reach-averaged slope varied from 0.07 to 0.11 for similar discharges/sand feed rates. This is caused by the internal dynamics of the system. In runs 9 and 10 for example, the difference is large, but the initial sand feed was slightly larger in Run 9 which reduced the initial gravel slope where sand began to interact with the bed. Gravel was more mobile and kept passing out of the flume, reducing the volume of gravel deposited at the toe of the gravel wedge and increasing the slope. Critically, the initial transport conditions were the same, with a stable gravel bed at the threshold of motion, regardless of the calculated slope.

3.2. Effect of a Grain Size Gap Feed on a Stable GST (Runs 9–12)

Adding a feed of FGG (2.8–5.6 mm) in Run 9 resulted in destabilization of the stable GST and gravel wedge. The GST progressively migrated downstream to the end of the flume over 20 min, but large quantities of previously immobile gravel particles were transported across the GST and rafted out of the flume. The GST did not re-establish with a sand bed downstream. The FGG gravel feed infiltrated to a depth equivalent to 2–3 bed material grain diameters (Figure 2a). The gravel bed changed from a gravel-sand mixture with a gravel mode at 9.8 mm and ~15% sand to a mixture with distinct modes at 0.57, 3.8, and 9.8 mm (trimodal) and a median of the gravel modes (nominal gravel D_{50}) of 5.1 mm (Figure 3a). Despite the GST having prograded to the end of the flume, some gravel particles continued to raft through the flume even after 5 min suggesting that the gravel bed had not fully achieved equilibrium. The final bed τ^*(0.0844) remained elevated above the slope-dependent τ_c^* (0.068) suggesting that some marginal transport should occur. The sand content of the gravel bed surface increased to 20%, while the proportion of FGG gravel on the final bed was 47%. The gravel reach water surface gradient reduced from 0.114 to 0.034, while u_r^* values reduced from 0.12 to 0.07 m/s (Table 2). Sand was carried as washload in the gravel reach before the perturbation caused by the 2.8–5.6 mm gravel addition, but as suspended bed material after the perturbation because u_r^*/ω reduced from 1.49 to 0.92 after the perturbation (Table 2).

Feeding CGG gravel onto the coarser NGG bed in Run 10 did not result in the same degree of destabilization of the GST as in Run 9. A smaller quantity of initial NGG bed material was rafted out of the flume. Most of the CGG feed deposited on the surface of the gravel wedge causing aggradation (Figure 2b) and resulting in a stable downstream advance of the GST (i.e., the initial gravel bed remained largely immobile). After ~13 min the GST had migrated to the end of the flume and the gravel bed was stable. This was also suggested by the final bed τ^*(0.053) which was lower than the slope-dependent τ_c^* (0.070) of the final bed. The proportion of CGG material on the final bed was ~21% with ~42% sand cover, based on the digitization of overhead photos. The bed surface changed from gravel to a sand-gravel mixture with a gravel mode at 8.8 mm (Figure 3b). A small quantity of the previously immobile NGG gravel bed rafted out of the flume (523 g in total), but most mobilized particles were re-deposited further down the gravel wedge, causing the GST to advance. This is consistent with exited mass measurements (Table 3) where CGG was net retained within the flume (equivalent to 0.65 g/s) where 67% of the total feed was deposited within the flume. The gravel reach gradient reduced from 0.084 to 0.048, while u_r^* reduced from 0.10 to 0.08 m/s (Table 2). As in Run 9, sand was carried as washload before the CGG gravel addition in the gravel reach, but changed to suspended bed material after the perturbation that caused u_r^*/ω to reduce from 1.27 to 0.70 (Table 2). Over the duration of Run 10, there was a net output of sand (0.97 g/s; Table 3), suggesting that sand was entrained from the initial equilibrium bed.

Mixing CGG (5.6–8 mm) into the initial bed and feeding in sand and FGG material (2.8–5.6 mm) in Run 11 resulted in advance of the GST, although the bed did not mobilize as dramatically as in Run 9 when there was no CGG material in the initial bed. After ~14 min, the GST migrated to the end of the flume and the gravel bed stabilized. The final bed τ^*(0.046) which was lower than the slope-dependent τ_c^* (0.063) of the final bed. The proportion of FGG (from the feed) and CGG material in the final bed was 42% in comparison to 39% CGG in the initial bed, NGG gravel coverage reduced to 27% from 46%, and the final sand cover was 31% (Figure 4a). Over the duration of the run, 114 and 161g of NGG and CGG material exited the flume, respectively, despite no feeds

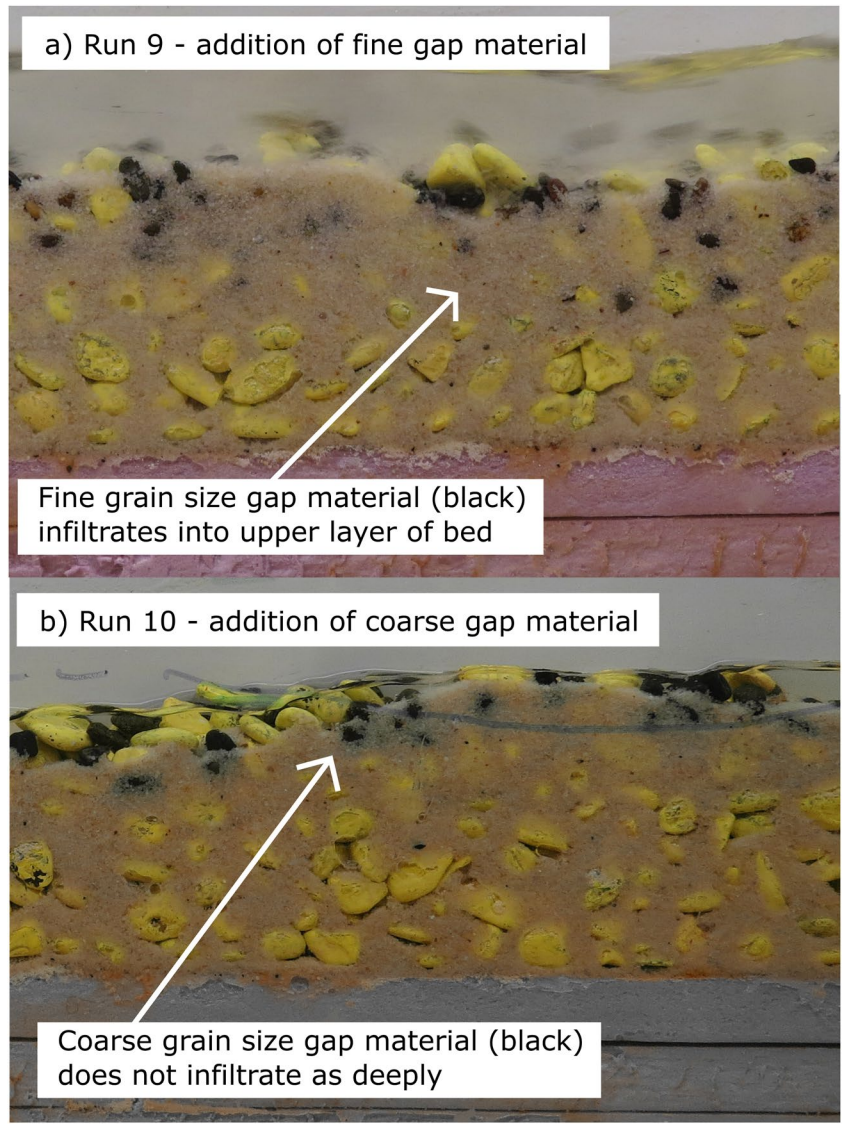

Figure 2. Side view of final bed in (a) Run 9 and (b) Run 10.

of these sizes. There was a net retention of FGG material, with 84% of the feed retained (net retention of 0.84 g/s; Table 3) and 39% of the sand feed also being retained. The initial gravel reach bed material was gravel with sand only present in interstitial spaces, with the gravel mode at 8.2 mm. The final gravel reach was bimodal with modes at 0.57 mm and a broad gravel mode with a nominal D_{50} of 7.1 mm (Figure 3c), although this is based on the assumption that final proportions of FGG and CGG are both 50%. The gravel reach gradient reduced from 0.069 to 0.032, while u_r^* reduced from 0.09 to 0.06 m/s (Table 2). Our observations of transport mode indicate the sand was transported as washload in the gravel reach before the perturbation, even though $u_r^*/\omega = 1.17$, marginally less than the threshold of 1.2, but there was a substantial decrease in u_r^*/ω after the perturbation to 0.80, indicating sand was moving as suspended bed material load after the perturbation which was consistent with observations (Table 2).

Feeding CGG gravel and sand in Run 12 onto the same bed as Run 11 resulted in bed aggradation and advance of the GST. After ~15 min, the gravel front reached the end of the flume and the gravel bed stabilized. This was also confirmed by the final bed $\tau^*(0.041)$ which was lower than the slope-dependent τ_c^* (0.067) of the final bed. The initial gravel bed remained relatively immobile, with most of the CGG gravel feed depositing on the gravel wedge surface or at the GST. After the perturbation, the sand fraction increased to 30% sand and the nominal D_{50} of the gravel mode reduced from 8.2 to 7.1 mm (Figure 3d). The proportion of CGG material in the bed

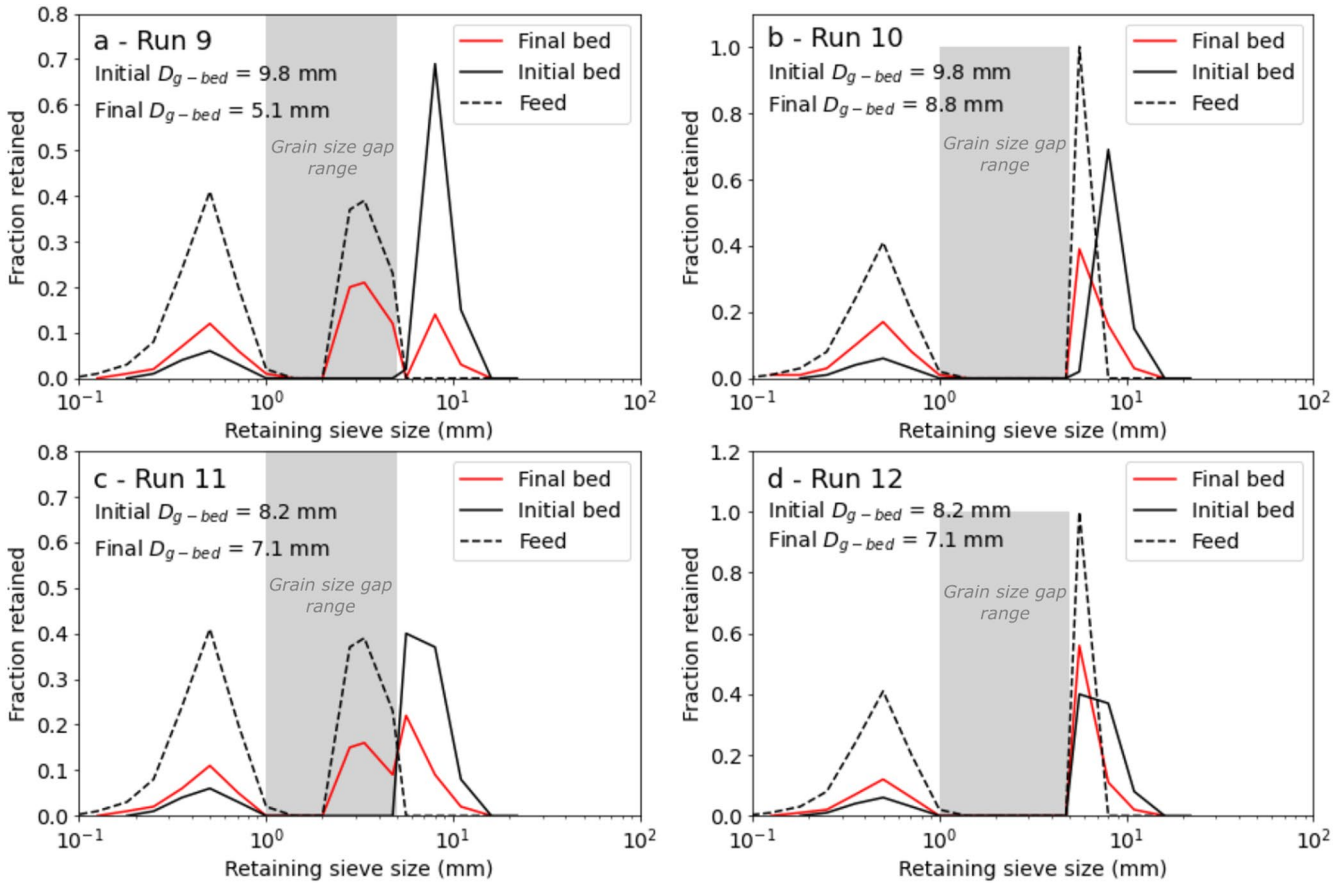

Figure 3. Changes in gravel reach bed grain size distributions for (a) Run 9 (added fine gap material to feed), (b) Run 10 (added coarse gap material to feed), (c) Run 11 (added coarse gap material to the bed and fine gap material to feed), and (d) Run 12 (added coarse gap material to the bed and feed).

increased from 39% to 56%, while the proportion of NGG gravel reduced to 14%. A small quantity of the initial bed material rafted out of the flume. The gravel reach gradient reduced from 0.062 to 0.039, while u_r^* reduced from 0.08 to 0.07 m/s (Table 2). Sand was observed being transported as washload in the gravel reach before the perturbation, but u_r^*/ω was marginally less than 1.2. As with the previous run, u_r^*/ω reduced substantially from 1.08 to 0.84 (Table 2), suggesting sand shifted from washload to being transported as suspended bed material load in the perturbed state.

3.2.1. GST Migration and Bed Mobilization in Runs 9–12

The degree to which the bed destabilized and the duration it took for the GST to prograde to the end of the flume varied across Runs 9–12. While measured sediment fluxes out of the flume are not available for Runs 9 and 12, the % change in the volume of the gravel wedge in the flume can be calculated using the change in longitudinal bed profile (Table 4).

There is an overall net loss in the volume of the gravel wedge in Run 9 (−6%), which is indicative of an overall net loss of gravel from the flume during the run (Table 4). At the upstream end of the gravel wedge, there was 4.4 cm of surface lowering. The addition of the FGG feed destabilized much of the gravel reach, and it took a longer time for the GST to migrate to the end of the flume (~20 min) as the gravel bed was so unstable.

In contrast, for Runs 10–12 some proportion of the sediment feed was retained within the flume. This is consistent with input and output measurements in Runs 10 and 11 (Table 2), where 299g (2 g/min) and 415g (30 g/min) of gravel were retained in the flume, respectively. In Run 10, there was a small amount of gravel mobilized from the upstream end of the wedge (surface lowering by a maximum of 2.7 cm), and to a lesser degree in Run 11 (surface lowering by a maximum of 1.2 cm). In Run 12, there was little net change in the gravel wedge volume. Visually, the bed on Run 12 was quite stable and the CGG feed was transported to the toe of the gravel wedge, resulting in

Table 3
Sediment Feeds, Outputs and % Retention for Sand and Gravel Fractions in Runs 9–16

Run ID	Run duration (s)	Sand	Fine grain gap	Coarse grain gap	Other sizes
Run 9[a]					
Total Feed (g)/Total Output (g)	1,228	4,859/-	1,218/-	0/-	0/-
Run 10					
Total Feed (g)/Total Output (g)	870	3,306/4,153	–	844/280	0/523
Net output (g/s) and % of feed		0.97 (25% lost)[b]	–	−0.65 (67% retained)[c]	0.60
Run 11					
Total Feed (g)/Total Output (g)	829	3,135/1,905	825/135	0/161	0/114
Net output (g/s) and % of feed		−1.49 (39% retained)	−0.84 (84% retained)	0.20	0.14
Run 12[a]					
Total Feed (g)/Total Output (g)	900	3,420/-	0	1,044/-	0/-
Run 13					
Total Feed (g)/Total Output (g)	3,480	13,746/11,139	0/0	0/2,965	0/0
Net output (g/s) and % of feed		−0.75 (19% retained)	0	0.85	0
Run 14					
Total Feed (g)/Total Output (g)	3,720	14,694/13,406	0/6,308	0/0	0/0
Net output (g/s) and % of feed		−0.35 (9% retained)	1.70	0	0
Run 15					
Total Feed (g)/Total Output (g)	5,040	19,908/16,723	0/364	0/491	0/814
Net output (g/s) and % of feed		−0.63 (16% retained)	0.07	0.10	0.16
Run 16					
Total Feed (g)/Total Output (g)	1,470	5,807/4,351	0/206	0/38	0/39
Net output (g/s) and % of feed		−0.99 (25% retained)	0.14	0.03	0.03

[a]Output measurements are not available for Runs 9 and 12. [b]Positive net output values represent the net rate at which sediment exited the flume, where the total output > total feed. [c]Negative net output values represent the net rate at which sediment was deposited within the flume where the total output < total feed.

a stable downstream advance of the GST. Some gravel at the upstream end of the wedge was mobilized (a maximum depth of 1.9 cm), and most of the sediment feed bypassed the wedge and exited the flume. The duration of Runs 10–12 were comparable (~14–15 min) and the bed did not dramatically destabilize.

3.3. Effect of Grain Size Gap Material in the Bed on Mobility (Runs 13 and 14)

Initially, Runs 13 and 14 were set up like other runs where we developed a gravel wedge in the upstream end of the flume made of grain size gap fractions that were at the threshold of motion. A sand feed was then started in an attempt to form a stable GST, as in Runs 9–12. However, when the sand feed was turned on, the wedge immediately mobilized and it was not possible to form a stable GST as the gravel rafted out of the flume. We were unable to build a sand reach in these runs. Runs 13 and 14 were therefore modified such that they started with the entire flume filled with grain size gap material to form a gravel wedge that was left to stabilize to the imposed Q without a sand feed. The initial flow conditions were not able to sustain sand as washload, but were able to maintain suspended bed material load ($u_r^*/\omega < 1.2$; Table 2). The Shields number was marginally below the threshold of motion for the gravel bed ($\tau^* = 0.048$ and $\tau_c^* = 0.065$). When the sand feed was turned on, the FGG and CGG gravel beds mobilized and large quantities of gravel were rafted out of the flume. This can be predicted by models for mixed sized sediment (Wilcock, 1998; Wilcock & Crowe, 2003; Wilcock & Kenworthy, 2002), but there is a preferential mobilization of grain size gap material in both runs.

With the CGG bed (5.6–8 mm) in Run 13, the proportion of sand on the bed surface increased to ~60% within the first 5 min of the sand feed and sand feed infiltrated into the upper few grains of the bed (Figure 5). The proportion of sand on the bed then slowly increased over the next 50 min to ~84% (Figure 6a). At this point, the bed

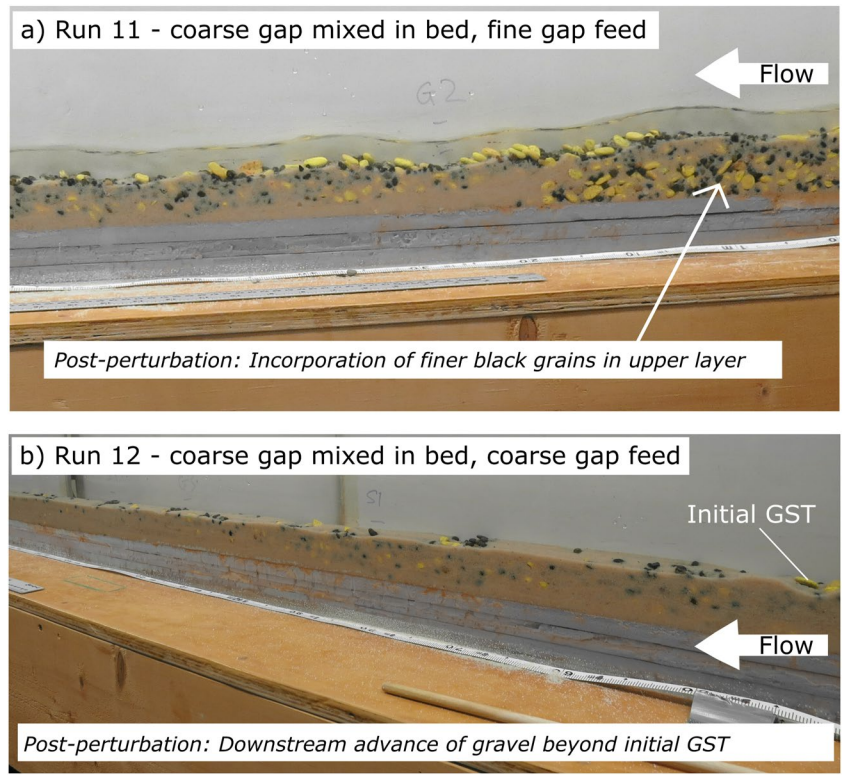

Figure 4. Final bed conditions in (a) Run 11 and (b) Run 12.

fully stabilized and gravel stopped exiting the flume. Over the duration of the run, 13.7 kg of sand was fed into the flume, while only 11.1 kg exited, suggesting a mass equivalent to ~19% of the total sand feed was retained within the flume (net retention of 0.75 g/s). Despite no gravel feed, 2.97 kg of gravel (that was initially immobile) was also evacuated from the flume (Figure 6a) at a rate of 0.85 g/s.

The initial condition for Run 14 was a bed composed of FGG grains. The flow was sufficient to produce a condition where the sand was carried as suspended bed material load ($u_r^*/\omega < 1.2$; Table 2). The FGG bed had a Shields number of 0.071 which is slightly higher than the slope-dependent τ_c^* value of 0.062, but our observations were that the bed was not mobile and there was no transport. The addition of the sand feed mobilized the FGG bed and to a greater degree than the CGG bed in Run 13. A smaller proportion (~9%) of the total sand feed was retained within the flume over the duration of the run (62 min). More than double the amount of FGG gravel (>6 kg) was evacuated from the flume in comparison to CGG gravel in Run 13 and at a higher rate of 1.70 g/s, despite no gravel feed. Within 5 min, more than 60% of the bed surface was sand, and rates of sand output were comparable to that of the sand feed (Figure 6b). After ~20 min, the FGG gravel output visually reduced, while sand output from the flume continued to fluctuate between 3 and 4 g/s. The sand content of the bed gradually increased to ~88% over the next ~50 min, after which gravel ceased exiting the flume. Net sand retention rates were lower in Run 14 than for Run 13 (0.35 and 0.75 g/s, respectively).

Table 4
Gravel Wedge Volumetric Changes in Run 9–12

Run ID	Run description	Initial/final gravel wedge volume (cm^3)	% Change	Gravel net retention rate
Run 9	FGG feed onto a stable GST (NGG gravel bed)	5,694/5,364	−6%	–
Run 10	CGG feed onto a stable GST (NGG gravel bed)	6,919/7,166	+4%	2 g/min
Run 11	FGG feed onto a stable GST (NGG + CGG gravel bed)	5,130/6,015	+17%	30 g/min
Run 12	CGG feed onto a stable GST (NGG + CGG gravel bed)	6,017/6,041	+0.4%	–

Note. The net gravel retention rate is included for Runs 10 and 11 where sediment output was directly measured for comparison.

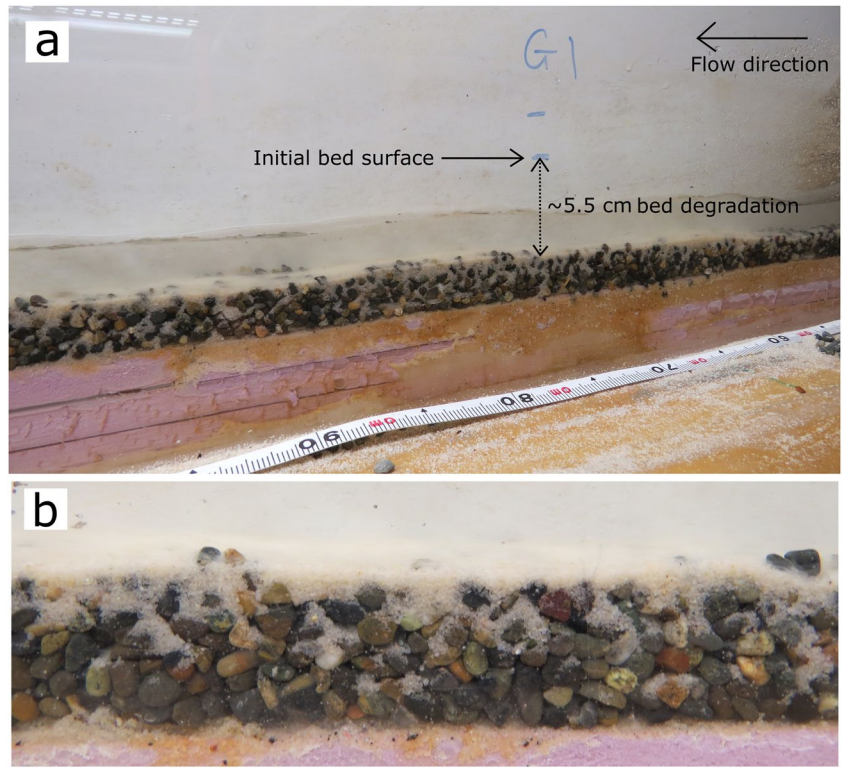

Figure 5. (a) Change in bed elevation at the upstream end of the flume when adding sand onto a stable FGG bed in Run 14. (b) Cross-section of the bed after 32 min in Run 14 where sand has only infiltrated ~3 grain diameter depth into the bed.

3.4. Effect of Grain Size Gap Material in Broader Bed Distributions on Mobility (Runs 15 and 16)

In Runs 15 and 16, we initially filled the flume entirely with gravel as in Runs 13 and 14. The flow was turned on and the gravel bed adjusted to a near threshold condition and particles were observed to be immobile. In Run 15, the initial gravel bed τ^* was 0.045 ($\tau_c^* = 0.064$), while in Run 16 τ^* was 0.110. For Run 16, this value is

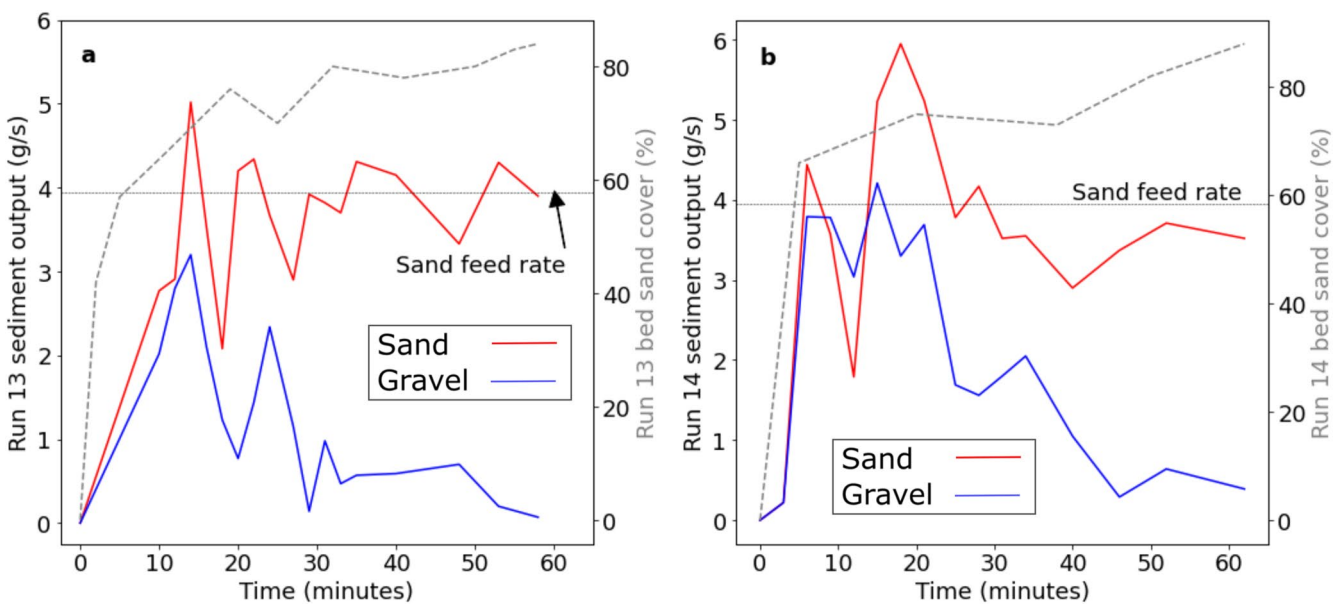

Figure 6. The sediment output for (a) Run 13 and (b) Run 14. Changes in bed surface % sand content are shown by the dashed gray line.

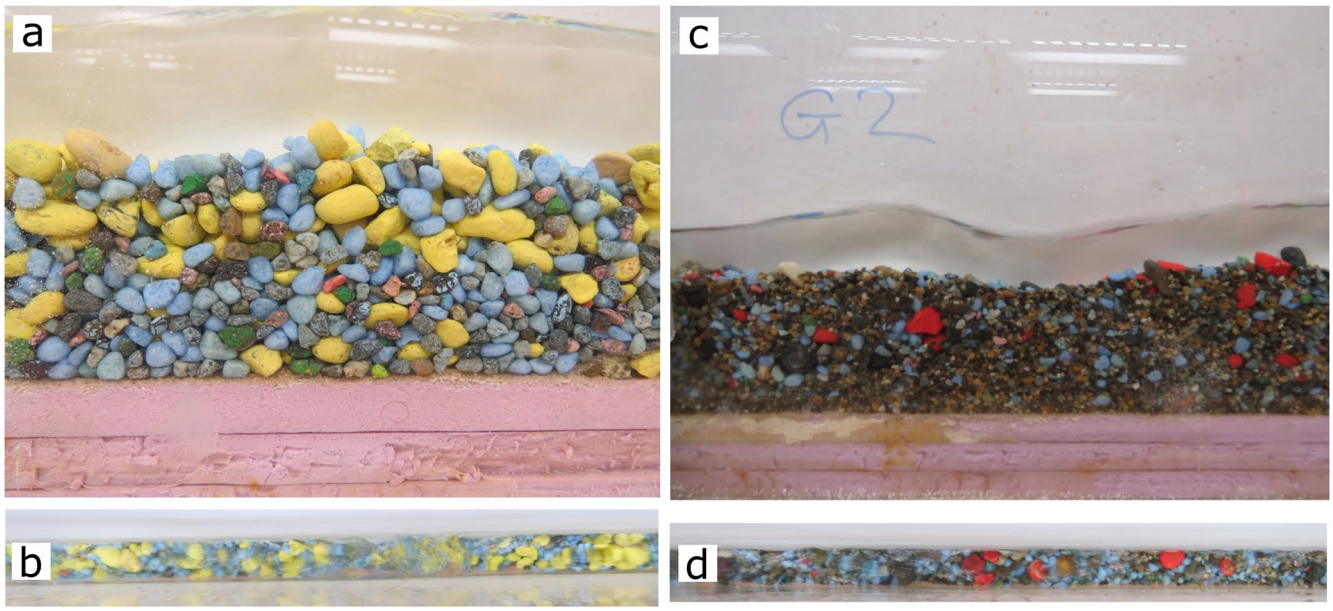

Figure 7. Cross-section and top-down view of the initial bed condition (a) and (b) Run 15 using 4–16 mm gravel and (c) and (d) Run 16 using 2–22 mm gravel.

considerably above the slope-dependent threshold of initial motion ($\tau_c^* = 0.074$), suggesting the bed had developed stable configurations of particles, reducing transport rates (e.g., Church et al., 1998). The coarsest grains used in Run 16 formed clusters approximately every 30 cm prior to the sand feed being turned on, generating small scour pools immediately downstream of each cluster that are similar to step-pool featured formed by particle jamming (e.g., Zimmermann et al., 2010). In the upper half of the flume, the pools were ∼5 cm deep, while in the lower half, they were shallower at ∼1 cm.

Feeding sand onto a 4–16 mm gravel bed (Figures 7a and 7b) in Run 15 resulted in a small mobilization of the gravel bed. Sand was transported as suspended bed material load ($u_r^*/\omega < 1.2$; Table 2). Over the duration of the run, 19.9 kg of sand was fed into the flume and 16.7 kg exited, suggesting ∼16% of the total sand feed was retained in the flume (net retention of 0.63 g/s). Despite no gravel feed, 1.7 kg of gravel (that was initially immobile) was evacuated from the flume (Figure 8a). The gravel became immobile when the bed was largely covered by sand (34%–50%), with some patches of gravel still visible after ∼84 min. The grain size distribution of material rafted out of the flume was nearly identical to that of the initial bed surface (Figure 8c). We calculated the grain size fraction in the bedload (P_i) relative to the fraction in the initial bed surface (F_i) and found that the bed surface distribution was well represented in the bedload (Figure 8e), which is an equal mobility condition with respect to the bed surface (Parker, 2008).

Feeding sand onto a 2–22 mm gravel distribution in Run 16 (Figures 7c and 7d) resulted in the formation of a weakly defined GST. In the upper half of the flume, the percentage sand cover on the final bed was <30% and sand was visually carried as washload in the upper half of the flume where u_r^*/ω was 1.23. In the lower part of the flume, there was 50%–60% sand coverage on the final bed and sand was visually carried as suspended-bed material load where u_r^*/ω values were also 0.87. Once the sand feed began, the shallower scour pools formed by coarse particle jamming initially deepened as finer material was remobilized and then filled with sand and partially buried the coarser clusters of gravel.

Some gravel was mobilized by the sand feed (Figure 8b). Over the duration of the run, 5.8 kg of sand was fed into the flume and 4.3 kg exited, suggesting ∼25% of the total sand feed was retained in the flume with a net retention rate of 0.99 g/s. Despite no gravel feed, 0.3 kg of gravel was evacuated from the flume. After ∼25 min, the bed was immobile again. The grain size distribution of the material transported out of the flume differed from the initial bed (Figure 8d) suggesting enhanced mobility of the FGG particles. The fractional mobility of FGG gravel was greater than the proportion of those sizes on the bed surface ($P_i/F_i > 1$) and 11–22 mm particles were underrepresented in the bedload compared to the surface size distribution ($P_i/F_i < 1$) (Figure 8f). This created a selective mobility regime (Parker, 2008) that depleted the bed of grain size gap material, primarily 2–5.6 mm particles.

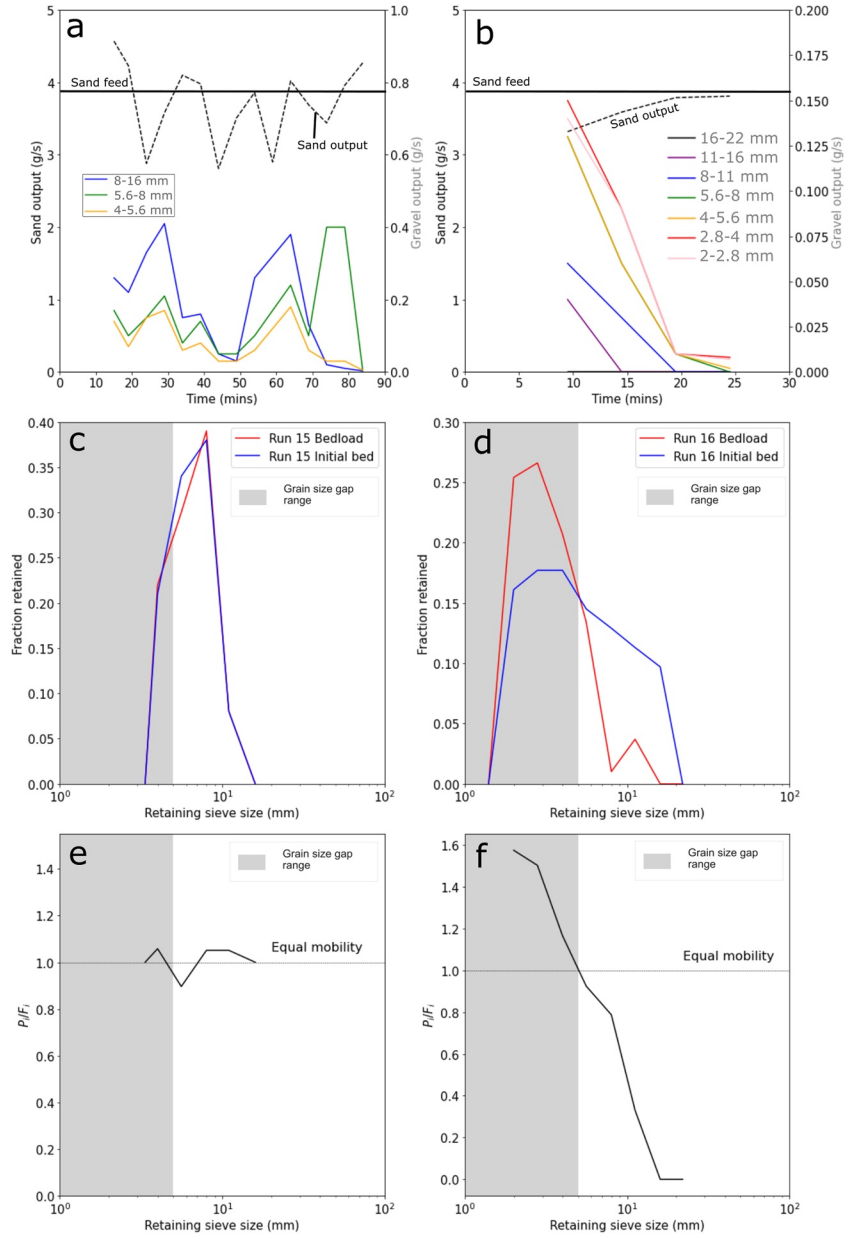

Figure 8. The sediment output for sand and gravel fractions in (a) Run 15 and (b) Run 16. Initial bed surface grain size distribution and measured bedload transported out of the flume in (c) Run 15 and (d) Run 16. The ratio of bedload (P_i) to the initial bed surface (F_i) for each grain size fraction in (e) Run 15 and (f) Run 16. Sand is not included in these distributions.

4. Discussion

4.1. Can GSTs Be Produced With Grain Size Gap Gravel Present in the Bed and Feed?

Dingle and Venditti (companion paper, 2023) undertook an experiment where a gravel wedge at the threshold of motion was created, then sand was fed into the flume and carried as washload through the gravel reach but deposited further downstream to create a sand bed reach. These experiments did not include grain size gap particles in the gravel bed or feed grain size distributions because they are rarely observed at GSTs. We were still able to create a GST using narrowly graded gravel with median sizes of 8 and 10 mm (the coarse end of the grain size gap) and a sand feed (Runs 9–12). Initially sand was carried as washload in the gravel reach, but adding a second feed composed of FGG or CGG gravel (D_{50} = 3.8 or 6.8 mm) destabilized the gravel wedge, creating a gravel-sand mixture with sand being transported as a suspended bed material load through the entire

length of the flume. Reductions in gravel bed gradient in Runs 10–12 appear to be driven by the deposition of sediment feed on the lower half of the gravel wedge surface (leading to a net increase in wedge volume), rather than major remobilization of the gravel bed surface (leading to a net decrease in wedge volume) as was noted in Run 9. As FGG material was fed onto the gravel wedge in Run 9, the gravel bed surface mobilized, resulting in mixing of the FGG feed into the active layer. The mixing of these two grain size populations should also result in an overall fining of the gravel mode $D_{50,}$ and lowering of the reach gradient, as well as τ_c^*, by extension. This is consistent with our observations where the reduction in gravel bed gradient was greatest in Run 9 (63% reduction) in comparison to Runs 10–12 (43%, 54%, and 37%, respectively) and the overall reduction in gravel grain size was also largest (>4 mm). Even when gravel had prograded to the end of the flume in Run 9, the bed never fully stabilized (i.e., individual gravel grains were intermittently mobile) where the final bed $\tau^* = 0.084$ and slope-dependent $\tau_c^* = 0.068$. The % volume change may be underestimated for Run 9. In Runs 10–12, the bed did not destabilize to the same degree and instead the FGG/CGG feed was either deposited on the surface of the gravel wedge or transported to the GST. In these runs, the overall change in gravel mode D_{50} was ∼1 mm. Our experiment suggests that it is possible to generate a stable GST with grain size gap material in the sediment feed (and with CGG mixed into the gravel bed) but adding the same size gravel feed resulted in different behaviors depending on the grain size of the initial gravel bed (e.g., Runs 9 and 11).

Importantly, our attempts to create a stable GST with just grain size gap material in the initial gravel bed (FGG and CGG) and a sand feed also failed (Runs 13 and 14). When grain size gap gravel is at the threshold of motion, sand could not be suspended as washload and instead was carried as suspended bed material load. As it starts to interact with the grain size gap gravel bed, the gravel bed becomes mobile. This effect was even more pronounced when the FGG material was within a broader bed distribution (Run 16). Turning on the sand feed produces a selective mobility regime and there is enhanced transport of FGG grain sizes relative to other gravel. Church and Hassan (2023) suggested that the grain size gap is created during bedload transport by enhanced mobility of the gap material relative to coarser grain sizes. Our experiments show that FGG particles can be depleted from gravel beds where sand is depositing from suspension from the same hydraulic removal effect. Mixed size sediment transport models (e.g., Wilcock & Crowe, 2003) would predict an increase in transport as sand is added to a gravel mixture, but they do not predict the preferential mobility of the FGG sized material, relative to other sizes.

Our experiment shows that stable gravel beds composed of material in the grain size gap range become mobile in the presence of sand. A similar effect is noted when grain size gap material is fed onto a coarser gravel bed. Combined, these observations point to a geometric effect between the gravel bed and feed grain sizes. When the sediment supply is moderately finer than the bed ($2 < D_* < 20$), the finer supply infiltrates and bridges the pores of the gravel bed, forming a layer of fine material near the surface (Dudill et al., 2017, 2020; Hill et al., 2017). The presence of finer sediment on a coarser gravel bed produces a hydraulic smoothing effect when pockets fill with finer material (Venditti et al., 2010b). Sand on gravel beds reduces the threshold entrainment stress, an effect that is captured in bedload transport models (Wilcock & Crowe, 2003), but the effect of finer sediment mobilizing a gravel bed is not limited to sand and also happens when finer gravel is added to coarser gravel (cf. Venditti et al., 2010a).

In order to compare the mobilization we observe in our experiments with observations of the effect of fine sediment on gravel beds, we calculate D_g^* as the ratio of the gravel size in the bed ($D_{g\text{-bed}}$) and the gravel supply ($D_{g\text{-sup}}$) (Table 5). We also calculate the D_s^* as the ratio of $D_{g\text{-bed}}$ and the sand supply ($D_{s\text{-sup}}$) (Table 5). When $D_g^* < 2$ the bed is generally immobile and instead aggrades, forcing the GST to migrate downstream because the gravel supply is too coarse to fill surficial pockets between gravel particles on the bed surface. When the sediment supply is somewhat finer, $D_g^* > 2$, an otherwise immobile bed is mobilized due to the hydraulic smoothing effect. The effect is greater when D_g^* is larger because the fine gravel more effectively fills the pockets of the coarser gravel bed. In Runs 9–12, a negative change in gravel wedge mass was observed only in Run 9, suggesting that this was the only run where the reduction in gravel bed gradient was driven by bed mobilization rather than bed aggradation in the lower half of the flume, which would have increased the gravel wedge volume. Out of the first four runs, D_g^* was highest in Run 9 (Table 5), where only Run 9 and Run 11 had a $D_g^* > 2$. The exact value or boundary of D_g^* at which this effect becomes apparent is difficult to discern from our data, owing to the spread of D_g^* values used. Nevertheless, the change in $D_{g\text{-bed}}$ also differed somewhat between Run 9 and Run 11 (>4 and 1 mm, respectively) despite only a small difference in D_g^*, suggesting that hydraulic smoothing of the bed became important in controlling the morphological response as D_g^* increased from 2.2 to 2.6.

Table 5
Effect of Gravel and Sand Supply on Gravel Bed Dynamics

Run ID	Gap material location	$D_{g\text{-bed}}$ (mm)	$D_{g\text{-feed}}$ (mm)	$D_{s\text{-feed}}$ (mm)	D_g^*	D_s^*	Outcome of additional feed (and net rate of >2.8 mm particle output)	% FGG/CGG/NGG in gravel output
Run 9	Feed	9.8	3.8	0.57	2.6	17.2	Unstable GST	–
Run 10	Feed	9.8	6.8	0.57	1.4	17.2	Stable GST (−2 g/min)	0/35/65
Run 11	Bed/Feed	8.2	3.8	0.57	2.2	14.4	Slightly unstable GST (−30 g/min)	33/39/28
Run 12	Bed/Feed	8.2	6.8	0.57	1.2	14.4	Stable GST	–
Run 13	Bed	6.8	n/a	0.57	n/a	11.9	Gravel mobilized (51 g/min)	0/100/0
Run 14	Bed	3.8	n/a	0.57	n/a	6.7	Gravel mobilized (101 g/min)	100/0/0
Run 15	Bed	7.7	n/a	0.57	n/a	13.5	Some gravel mobilized (20 g/min)	22/29/49
Run 16	Bed	5.5	n/a	0.57	n/a	9.6	Only fine gravel mobilized (12 g/min)	73/13/14

4.2. Why Does Sand Cause Selective Entrainment of Gap Gravel?

The effect of adding sand to a bed of grain size gap material results in the mobilization of the gravel bed because sand fills pockets on the surface. This produces a bridging effect where further additions of sand cannot percolate, producing the aforementioned hydraulic smoothing effect. In our experiments when $D_s^* < 10$, the bed is composed either entirely or partially of FGG material and the mobilization effect is greatest (Table 5), because the sand more effectively fills gaps between the FGG gravel enhancing the hydraulic smoothing effect. This effect is most apparent in Run 14 where the rate of gravel exiting from the flume was highest (Table 5). When $D_s^* > 10$ the bed is made of CGG or NGG material (Table 5). The same mobilization effect occurs, but the smoothing effect appears to be lesser than for sand and FGG material in Runs 14 and 16. There appears to be some optimal ratio of D_s^* between $2 < D_s^* < 10$ where the hydraulic smoothing and gravel mobilization is most effective.

The distribution of gravel grain sizes in the bed matters in terms of mobilization. Although D_s^* is similar for the narrow gravel distribution and the wider gravel distribution in Runs 15 and 16, the effect is different. The narrow distribution that includes the CGG material is mobilized, but equal mobility occurs. The wider distribution in Run 16 is selectively mobile with the FGG sized material dominating the exited flux from the flume (Table 5). This presumably occurs because the sand is more effective at bridging the pockets formed by FGG gravel than for the coarser CGG gravel (e.g., Dudill et al., 2017, 2020), creating a differential mobility.

We suspect that the effect of both sand and gravel on bed mobilization is a geometric effect that is most effective where the ratio of grain sizes in the supply and the bed optimizes the hydraulic smoothing effect (Venditti et al., 2010a). Our results and other experiments (e.g., Dudill et al., 2017, 2020; Hill et al., 2017) suggest an optimal ratio to mobilize gravel beds that naturally exist in river systems for medium sand and FGG gravel. There are no other documented abrupt grain size transitions in the fluvial system, yet there are a wide variety of sizes that mix in the fluvial system. This begs for investigation of why the mobilization effect does not occur for larger sediment sizes with the same optimal D_* ratio. Recent work by Parker et al. (2023) proposed that fine gravel in the FGG range should be preferentially transported as bedload over a finer sand bed, relative to the same D_* ratio outside of this absolute range, because of a viscosity driven hydrodynamic smoothing effect. They argued that as the sand fraction of the bed increases and the bed transitions from a turbulent rough to turbulent smooth boundary condition, viscosity becomes relevant to the entrainment and transport of FGG gravel through lowering of the threshold Shields number (Novak & Nalluri, 1975).

4.3. Morphological Consequences of Washload Deposition and Hydraulic Sorting on Grain Size Gap Particles at the GST

Our experiment was designed to focus on a particular set of phenomena relating to the behavior of the grain size gap material and hydraulic sorting of grain sizes in the sand and fine gravel ranges. We cannot rule out the possibility of other contributing factors (e.g., hydraulic sorting of bimodal hillslope grain size sediment supply) that could result in the development of GSTs in particular landscapes (e.g., Dingle et al., 2021). Nevertheless, our experiments provide insights into the particle dynamics that occur at the GST (Figure 9). The boundary shear stress applied to a river bed declines moving in the downstream direction resulting in downstream fining. As u_r^*

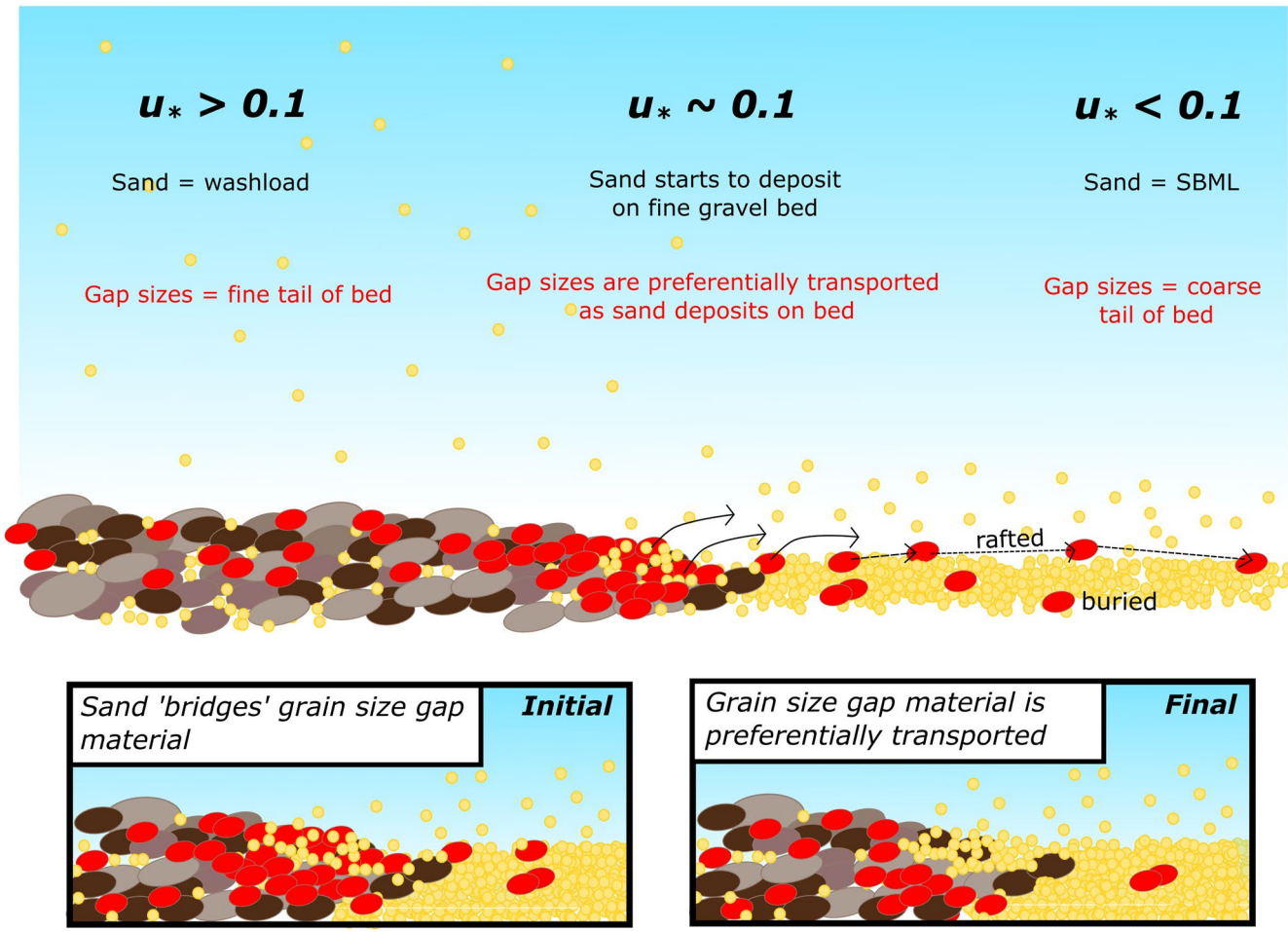

Figure 9. Schematic of enhanced mobility of grain size gap material (red grains) across the gravel-sand transition. Suspended bed material load = SBML).

reduces to ~0.1 m/s at the GST, fine gravel starts to deposit out of the bedload supply (Dingle & Venditti, 2023). Concurrently, deposition of sand from washload at $u_r^* = 0.1$ m/s enhances the mobility of FGG material on the bed surface and sharpens the grain size reduction across the GST.

As sand starts to deposit on grain size gap material on the bed surface at the GST, the mobility of the FGG material is enhanced due to a hydraulic smoothing effect. Medium sand grain sizes are too coarse to freely percolate deep into a FGG gravel framework, and instead bridge the upper layer of the bed filling the pockets of the gravel bed. Our experiment suggests that this observation remains valid even when FGG particles are present in broader gravel grain size distributions in sufficient quantity. Our experiment further suggests that this results in enhanced mobility of grain size gap material within the gravel bed surface, depleting this grain size fraction from the surface distribution. The diffuse extension (Venditti & Church, 2014; Venditti et al., 2015) represents a reach in which D_* adjusts to this change in bed and sediment supply grain size initiated by sand rapidly falling out of suspension at the upstream end of the GST.

Lamb and Venditti (2016) presented a theoretical basis for why mass deposition of medium sand grain sizes should occur at shear velocities of ~0.1 m/s, an effect that is specific to these grain sizes. They argued that the grain size gap occurs because fine gravel grain sizes are split between reaches upstream and downstream of the GST. Our experiment supports that hypothesis. Based on observations from our experiment, a logical development of this argument is that this rapid deposition of medium sand grain sizes initiates a geometric effect resulting in preferential mobility of FGG particles and subsequently their relative depletion from gravel bed distributions at the GST. The hydraulic sorting of bedload (Church & Hassan, 2023) may explain why the grain size gap exists upstream of GSTs in gravel bed rivers where washload deposition does not occur, but approaching

the GST the gap may be substantially enhanced by washload deposition. Grain size gap particles are transported across the GST where they remain in motion until they are either buried, find a resting space on the bed surface in the diffuse extension, or exit the fluvial system (Figure 9). Patches of gravel on the sand bed surfaces are common in sand bed reaches (e.g., Ferguson et al., 1989; Venditti & Church, 2014) creating the appearance of a diffuse extension to the GST observed in many rivers (Arbós et al., 2021; Frings, 2011; Singer, 2008, 2010; Venditti & Church, 2014; Venditti et al., 2015, 2019). These patches are ultimately buried as gravel lenses in sand deposits (Ferguson et al., 1989; Venditti & Church, 2014).

The ultimate fate of the grain size gap material in the fluvial system is also still not clear from our experiments. Deposition of gap material in the sand reaches of our experiment runs where GSTs were developed was limited. After crossing the GST, FGG material was rafted at the end of our flume (e.g., Run 9). We suspect that gap material may have a similar fate in many natural systems (e.g., Russell, 1968). Gravel particles can raft over sand beds because gravel protrudes above roughness elements on the bed and experiences the full force of near bed flow. Gravel within the grain size gap range may also experience enhanced relative mobility over a sand bed once passing through the GST because of the increasing dominance of effects relating to viscosity (in comparison to coarser gravel beds), leading to a dilution of grain size gap gravel within sand and finer grain size distributions (Parker et al., 2023). Where the GST is far upstream of lakes and marine environments, we suspect that fine gravel may diffuse into the sand bed over long distances until it is exhausted from the system. Where the GST occurs closer to lakes and marine environments, we suspect that gap material is transported through the fluvial system and into marine environments where deposits of gap gravel are more common (e.g., Jennings & Shulmeister, 2002; McLean, 1970; Russell, 1968).

Our experiment offers a new insight as to why rivers with beds composed of 1–5 mm gap gravel are so rare at Earth's surface. When medium sand is added to a gravel bed with 1–5 mm gravel present, the sand infiltrates, bridging the gaps between fine gravel particles, and smoothing the bed. This creates a selective mobility transport regime that depletes the gravel beds of 1–5 mm gravel. This can happen anytime that sand is supplied to a gravel bed and does not involve washload deposition. Our observations suggest that anywhere this interaction occurs, the bed will be depleted in 1–5 mm gravel. The ubiquity of medium sand in most watersheds means that beds composed primarily of fine grain size gap material should be very rare.

5. Conclusions

We undertook a series of flume runs documenting changes in fine gravel (<10 mm) transport across a stable GST. Feeding grain size gap material (2.8–8 mm) onto a coarser (∼10 mm) gravel bed reach mobilized the bed and destabilized the GST, leading to downstream advance of the GST. It was not possible to generate a stable GST with a gravel reach composed of grain size gap material, as the gravel bed would immediately mobilize once the sand feed was turned on. Sand could not be carried as a washload where grain size gap particles were below the threshold for entrainment. We find that gravel mobilization occurs when the ratio of the bed material and sediment supply size is between 2 and 20 and find evidence for an optimal ratio <10. Adding medium sand to a bed composed of a wider gravel size distribution causes enhanced mobility of 2–5.6 mm gravel. It is not possible to form stable gravel beds dominated by these grain sizes where sand is also present, which may help to explain the relative paucity of gravel beds dominated by ∼1–5 mm material in Earth's river systems.

Data Availability Statement

Details on all experiment parameters and primary data underlying the analysis are presented within the manuscript and are available in full in the Zenodo repository https://doi.org/10.5281/zenodo.6261166 (Dingle & Venditti, 2023).

Acknowledgments
Experiments, analysis and writing of this manuscript were supported through an NSERC Discovery Grant and Accelerator Supplement awarded to J.V. The authors are grateful to Kyle Kusack and Morgan Wright for their assistance in building and running the experiments, and to Mike Church for comments on the manuscript. The authors thank six anonymous reviewers and the Editors for their feedback, which has undoubtedly improved the manuscript.

References

An, C., Parker, G., Fu, X., Lamb, M. P., & Venditti, J. G. (2020). Morphodynamics of downstream fining in rivers with unimodal sand-gravel feed. In *River flow 2020*. CRC Press.

An, C., Parker, G., Hassan, M. A., & Fu, X. (2019). Can magic sand cause massive degradation of a gravel-bed river at the decadal scale? Shi-ting River, China. *Geomorphology*, *327*, 147–158. https://doi.org/10.1016/j.geomorph.2018.10.026

Ancey, C., & Pascal, I. (2020). Estimating mean bedload transport rates and their uncertainty. *Journal of Geophysical Research: Earth Surface*, *125*(7), e2020JF005534. https://doi.org/10.1029/2020JF005534

Arbós, C. Y., Blom, A., Viparelli, E., Reneerkens, M., Frings, R. M., & Schielen, R. M. J. (2021). River response to anthropogenic modification: Channel steepening and gravel front fading in an incising river. *Geophysical Research Letters*, *48*(4), e2020GL091338. https://doi.org/10.1029/2020GL091338

Bagnold, R. A. (1966). *An approach to the sediment transport problem from general physics*. U.S. Government Printing Office.

Benavides, S. J., Deal, E., Rushlow, M., Venditti, J. G., Zhang, Q., Kamrin, K., & Perron, J. T. (2022). The impact of intermittency on bed load sediment transport. *Geophysical Research Letters*, *49*(5), e2021GL096088. https://doi.org/10.1029/2021GL096088

Benavides, S. J., Deal, E., Venditti, J. G., Bradley, R., Zhang, Q., Kamrin, K., & Perron, J. T. (2023). How fast or how many? Sources of intermittent sediment transport. *Geophysical Research Letters*, *50*(9), e2022GL101919. https://doi.org/10.1029/2022GL101919

Blom, A., Chavarrías, V., Ferguson, R. I., & Viparelli, E. (2017). Advance, retreat, and halt of abrupt gravel-sand transitions in alluvial rivers. *Geophysical Research Letters*, *44*(19), 9751–9760. https://doi.org/10.1002/2017GL074231

Bridge, J. S. (2009). *Rivers and floodplains: Forms, processes, and sedimentary record*. John Wiley & Sons.

Carling, P. A., & Reader, N. A. (1982). Structure, composition and bulk properties of upland stream gravels. *Earth Surface Processes and Landforms*, *7*(4), 349–365. https://doi.org/10.1002/esp.3290070407

Church, M. (2006). Bed material transport and the morphology of alluvial river channels. *Annual Review of Earth and Planetary Sciences*, *34*(1), 325–354. https://doi.org/10.1146/annurev.earth.33.092203.122721

Church, M., & Hassan, M. (2005). Estimating the transport of bed material at low rate in gravel armoured channels. In R. J. Batalla, & C. Garcia (Eds.), *Geomorphological processes and human impacts on river basins* (pp. 141–153). IAHS.

Church, M., & Hassan, M. A. (2023). The fluvial grain-size gap: Experimental confirmation of hydraulic origin. *Earth Surface Processes and Landforms*, *48*(8), 1502–1511. https://doi.org/10.1002/esp.5562

Church, M., Hassan, M. A., & Wolcott, J. F. (1998). Stabilizing self-organized structures in gravel-bed stream channels: Field and experimental observations. *Water Resources Research*, *34*(11), 3169–3179. https://doi.org/10.1029/98WR00484

Church, M., Wolcott, J. F., & Fletcher, W. K. (1991). A test of equal mobility in fluvial sediment transport: Behavior of the sand fraction. *Water Resources Research*, *27*(11), 2941–2951. https://doi.org/10.1029/91WR01622

Church, M., & Zimmermann, A. (2007). Form and stability of step-pool channels: Research progress. *Water Resources Research*, *43*(3), W03415. https://doi.org/10.1029/2006wr005037

Cui, Y., & Parker, G. (1998). The arrested gravel front: Stable gravel-sand transitions in rivers Part 2: General numerical solution. *Journal of Hydraulic Research*, *36*(2), 159–182. https://doi.org/10.1080/00221689809498631

Curran, J. C., & Wilcock, P. R. (2005). Effect of sand supply on transport rates in a gravel-bed channel. *Journal of Hydraulic Engineering*, *131*(11), 961–967. https://doi.org/10.1061/(ASCE)0733-9429(2005)131:11(961)

Deal, E., Venditti, J. G., Benavides, S. J., Bradley, R., Zhang, Q., Kamrin, K., & Perron, J. T. (2023). Grain shape effects in bed load sediment transport. *Nature*, *613*(7943), 298–302. https://doi.org/10.1038/s41586-022-05564-6

Dingle, E. H., Attal, M., & Sinclair, H. D. (2017). Abrasion-set limits on Himalayan gravel flux. *Nature*, *544*(7651), 471–474. https://doi.org/10.1038/nature22039

Dingle, E. H., Kusack, K. M., & Venditti, J. G. (2021). The gravel-sand transition and grain size gap in river bed sediments. *Earth-Science Reviews*, *222*, 103838. https://doi.org/10.1016/j.earscirev.2021.103838

Dingle, E. H., Sinclair, H. D., Venditti, J. G., Attal, M., Kinnaird, T. C., Creed, M., et al. (2020). Sediment dynamics across gravel-sand transitions: Implications for river stability and floodplain recycling. *Geology*, *48*(5), 468–472. https://doi.org/10.1130/G46909.1

Dingle, E. H., & Venditti, J. G. (2023). Experiments on gravel-sand transitions. *Zenodo*. https://doi.org/10.5281/zenodo.6261166

Dudill, A., Frey, P., & Church, M. (2017). Infiltration of fine sediment into a coarse mobile bed: A phenomenological study. *Earth Surface Processes and Landforms*, *42*(8), 1171–1185. https://doi.org/10.1002/esp.4080

Dudill, A., Venditti, J. G., Church, M., & Frey, P. (2020). Comparing the behaviour of spherical beads and natural grains in bedload mixtures. *Earth Surface Processes and Landforms*, *45*(4), 831–840. https://doi.org/10.1002/esp.4772

Einstein, H. A. (1950). *The bed-load function for sediment transportation in open channel flows*. U.S. Department of Agriculture.

Einstein, H. A. (1968). Deposition of suspended particles in a gravel bed. *Journal of the Hydraulics Division*, *94*(5), 1197–1206. https://doi.org/10.1061/JYCEAJ.0001868

Elgueta-Astaburuaga, M. A., & Hassan, M. A. (2017). Experiment on temporal variation of bed load transport in response to changes in sediment supply in streams. *Water Resources Research*, *53*(1), 763–778. https://doi.org/10.1002/2016WR019460

Elgueta-Astaburuaga, M. A., & Hassan, M. A. (2019). Sediment storage, partial transport, and the evolution of an experimental gravel bed under changing sediment supply regimes. *Geomorphology*, *330*, 1–12. https://doi.org/10.1016/j.geomorph.2018.12.018

Elgueta-Astaburuaga, M. A., Hassan, M. A., Saletti, M., & Clarke, G. K. C. (2018). The effect of episodic sediment supply on bedload variability and sediment mobility. *Water Resources Research*, *54*(9), 6319–6335. https://doi.org/10.1029/2017WR022280

Ferguson, R., Hoey, T., Wathen, S., & Werritty, A. (1996). Field evidence for rapid downstream fining of river gravels through selective transport. *Geology*, *24*(2), 179–182. https://doi.org/10.1130/0091-7613(1996)024<0179:FEFRDF>2.3.CO;2

Ferguson, R. I. (2003). Emergence of abrupt gravel to sand transitions along rivers through sorting processes. *Geology*, *31*(2), 159–162. https://doi.org/10.1130/0091-7613(2003)031<0159:EOAGTS>2.0.CO;2

Ferguson, R. I., Bloomer, D. J., & Church, M. (2011). Evolution of an advancing gravel front: Observations from Vedder Canal, British Columbia. *Earth Surface Processes and Landforms*, *36*(9), 1172–1182. https://doi.org/10.1002/esp.2142

Ferguson, R. I., & Church, M. (2004). A simple universal equation for grain settling velocity. *Journal of Sedimentary Research*, *74*(6), 933–937. https://doi.org/10.1306/051204740933

Ferguson, R. I., Prestegaard, K. L., & Ashworth, P. J. (1989). Influence of sand on hydraulics and gravel transport in a braided gravel bed river. *Water Resources Research*, *25*(4), 635–643. https://doi.org/10.1029/WR025i004p00635

Flammer, G. H., Tullis, J. P., & Mason, E. S. (1970). Free surface, velocity gradient flow past hemisphere. *Journal of the Hydraulics Division*, *96*(7), 1485–1502. https://doi.org/10.1061/JYCEAJ.0002563

Frey, P., Lafaye de Micheaux, H., Bel, C., Maurin, R., Rorsman, K., Martin, T., & Ducottet, C. (2020). Experiments on grain size segregation in bedload transport on a steep slope. *Advances in Water Resources*, *136*, 103478. https://doi.org/10.1016/j.advwatres.2019.103478

Frings, R. M. (2011). Sedimentary characteristics of the gravel–sand transition in the River Rhine. *Journal of Sedimentary Research*, *81*(1), 52–63. https://doi.org/10.2110/jsr.2011.2

Garcia, M. (2008). *Sedimentation engineering*. American Society of Civil Engineers. https://doi.org/10.1061/9780784408148

Gibson, S., Abraham, D., Heath, R., & Schoellhamer, D. (2010). Bridging process threshold for sediment infiltrating into a coarse substrate. *Journal of Geotechnical and Geoenvironmental Engineering*, *136*(2), 402–406. https://doi.org/10.1061/(asce)gt.1943-5606.0000219

Gomez, B., Rosser, B. J., Peacock, D. H., Hicks, D. M., & Palmer, J. A. (2001). Downstream fining in a rapidly aggrading gravel bed river. *Water Resources Research*, *37*(6), 1813–1823. https://doi.org/10.1029/2001WR900007

Graham, D. J., Rice, S. P., & Reid, I. (2005). A transferable method for the automated grain sizing of river gravels. *Water Resources Research*, *41*(7), W07020. https://doi.org/10.1029/2004WR003868

Gran, K. B., Montgomery, D. R., & Sutherland, D. G. (2006). Channel bed evolution and sediment transport under declining sand inputs. *Water Resources Research*, *42*(10), W10407. https://doi.org/10.1029/2005WR004306

Hassan, M. A., Saletti, M., Johnson, J. P. L., Ferrer-Boix, C., Venditti, J. G., & Church, M. (2020). Experimental insights into the threshold of motion in alluvial channels: Sediment supply and streambed state. *Journal of Geophysical Research: Earth Surface*, *125*(12), e2020JF005736. https://doi.org/10.1029/2020JF005736

Hill, K. M., Gaffney, J., Baumgardner, S., Wilcock, P., & Paola, C. (2017). Experimental study of the effect of grain sizes in a bimodal mixture on bed slope, bed texture, and the transition to washload. *Water Resources Research*, *53*(1), 923–941. https://doi.org/10.1002/2016WR019172

Hoey, T. B., & Ferguson, R. (1994). Numerical simulation of downstream fining by selective transport in gravel bed rivers: Model development and illustration. *Water Resources Research*, *30*(7), 2251–2260. https://doi.org/10.1029/94WR00556

Ikeda, H., & Iseya, F. (1988). *Experimental study of heterogeneous sediment transport*. Environmental Research Centre, University of Tsukuba. (Paper 12).

Jackson, W. L., & Beschta, R. L. (1984). Influences of increased sand delivery on the morphology of sand and gravel channels 1. *JAWRA Journal of the American Water Resources Association*, *20*(4), 527–533. https://doi.org/10.1111/j.1752-1688.1984.tb02835.x

Jennings, R., & Shulmeister, J. (2002). A field based classification scheme for gravel beaches. *Marine Geology*, *186*(3), 211–228. https://doi.org/10.1016/S0025-3227(02)00314-6

Jerolmack, D. J., & Brzinski, T. A. (2010). Equivalence of abrupt grain-size transitions in alluvial rivers and eolian sand seas: A hypothesis. *Geology*, *38*(8), 719–722. https://doi.org/10.1130/G30922.1

Kodama, Y. (1994). Experimental study of abrasion and its role in producing downstream fining in gravel-bed rivers. *Journal of Sedimentary Research*, *64*(1a), 76–85. https://doi.org/10.2110/jsr.64.76

Kuhnle, R. A. (1993). Fluvial transport of sand and gravel mixtures with bimodal size distributions. *Sedimentary Geology*, *85*(1), 17–24. https://doi.org/10.1016/0037-0738(93)90072-D

Lamb, M. P., Brun, F., & Fuller, B. M. (2017). Direct measurements of lift and drag on shallowly submerged cobbles in steep streams: Implications for flow resistance and sediment transport. *Water Resources Research*, *53*(9), 7607–7629. https://doi.org/10.1002/2017WR020883

Lamb, M. P., de Leeuw, J., Fischer, W. W., Moodie, A. J., Venditti, J. G., Nittrouer, J. A., et al. (2020). Mud in rivers transported as flocculated and suspended bed material. *Nature Geoscience*, *13*(8), 566–570. https://doi.org/10.1038/s41561-020-0602-5

Lamb, M. P., Dietrich, W. E., & Venditti, J. G. (2008). Is the critical Shields stress for incipient sediment motion dependent on channel-bed slope? *Journal of Geophysical Research*, *113*(F2), F02008. https://doi.org/10.1029/2007JF000831

Lamb, M. P., & Venditti, J. G. (2016). The grain size gap and abrupt gravel-sand transitions in rivers due to suspension fallout. *Geophysical Research Letters*, *43*(8), 3777–3785. https://doi.org/10.1002/2016GL068713

Mason, R. J., Rice, S. P., Wood, P. J., & Johnson, M. F. (2019). The zoogeomorphology of case-building caddisfly: Quantifying sediment use. *Earth Surface Processes and Landforms*, *44*(12), 2510–2525. https://doi.org/10.1002/esp.4670

McLean, D. G. (1990). *The relation between channel instability and sediment transport on Lower Fraser River*. University of British Columbia. https://doi.org/10.14288/1.0302167

McLean, R. F. (1970). Variations in grain-size and sorting on two kaikoura beaches. *New Zealand Journal of Marine & Freshwater Research*, *4*(2), 141–164. https://doi.org/10.1080/00288330.1970.9515334

Miller, M. C., McCave, I. N., & Komar, P. D. (1977). Threshold of sediment motion under unidirectional currents. *Sedimentology*, *24*(4), 507–527. https://doi.org/10.1111/j.1365-3091.1977.tb00136.x

Niño, Y., Lopez, F., & Garcia, M. (2003). Threshold for particle entrainment into suspension. *Sedimentology*, *50*(2), 247–263. https://doi.org/10.1046/j.1365-3091.2003.00551.x

Niño, Y., Lopez, F., & Garcia, M. H. (1994). High-speed video analysis of sediment-turbulence interaction. In *Proceedings of the symposium on fundamentals and advancements in hydraulic measurements and experimentation*. (pp. 213–222).

Novak, P., & Nalluri, C. (1975). Sediment transport in smooth fixed bed channels. *Journal of the Hydraulics Division*, *101*(9), 1139–1154. https://doi.org/10.1061/JYCEAJ.0004412

Paola, C., Parker, G., Seal, R., Sinha, S. K., Southard, J. B., & Wilcock, P. R. (1992). Downstream fining by selective deposition in a laboratory flume. *Science*, *258*(5089), 1757–1760. https://doi.org/10.1126/science.258.5089.1757

Paola, C., Straub, K., Mohrig, D., & Reinhardt, L. (2009). The "unreasonable effectiveness" of stratigraphic and geomorphic experiments. *Earth-Science Reviews*, *97*(1–4), 1–43. https://doi.org/10.1016/j.earscirev.2009.05.003

Parker, G. (2008). Transport of gravel and sediment mixtures. In *Sedimentation engineering: Processes, measurements, modeling, and practice* (pp. 165–251). American Society of Civil Engineers.

Parker, G., An, C., Lamb, M. P., Garcia, M. H., Dingle, E. H., & Venditti, J. G. (2023). Dimensionless argument: A narrow grain size range near 2 mm plays a special role in river sediment transport and morphodynamics. *EGUsphere*, 1–19. https://doi.org/10.5194/egusphere-2023-1705

Parker, G., & Cui, Y. (1998). The arrested gravel front: Stable gravel-sand transitions in rivers Part 1: Simplified analytical solution. *Journal of Hydraulic Research*, *36*(1), 75–100. https://doi.org/10.1080/00221689809498379

Pascal, I., Ancey, C., & Bohorquez, P. (2021). The variability of antidune morphodynamics on steep slopes. *Earth Surface Processes and Landforms*, *46*(9), 1750–1765. https://doi.org/10.1002/esp.5110

Reid, S. C., Lane, S. N., Berney, J. M., & Holden, J. (2007). The timing and magnitude of coarse sediment transport events within an upland, temperate gravel-bed river. *Geomorphology*, *83*(1), 152–182. https://doi.org/10.1016/j.geomorph.2006.06.030

Rice, S. (1999). The nature and controls on downstream fining within sedimentary links. *Journal of Sedimentary Research*, *69*(1). https://doi.org/10.1306/d426895f-2b26-11d7-8648000102c1865d

Russell, R. J. (1968). Where most grains of very coarse sand and fine gravel are deposited. *Sedimentology*, *11*(1–2), 31–38. https://doi.org/10.1111/j.1365-3091.1968.tb00838.x

Sambrook Smith, G. H., & Ferguson, R. I. (1995). The gravel-sand transition along river channels. *Journal of Sedimentary Research*, *65*(2). Retrieved from http://archives.datapages.com/data/sepm/journals/v63-66/data/065a/065a002/0423.htm

Scheingross, J. S., Brun, F., Lo, D. Y., Omerdin, K., & Lamb, M. P. (2014). Experimental evidence for fluvial bedrock incision by suspended and bedload sediment. *Geology*, *42*(6), 523–526. https://doi.org/10.1130/G35432.1

Schmeeckle, M. W., Nelson, J. M., & Shreve, R. L. (2007). Forces on stationary particles in near-bed turbulent flows. *Journal of Geophysical Research*, *112*(F2), F02003. https://doi.org/10.1029/2006JF000536

Shaw, J., & Kellerhals, R. (1982). *The composition of recent alluvial gravels in Alberta river beds*. Alberta Research Council.

Singer, M. B. (2008). Downstream patterns of bed material grain size in a large, lowland alluvial river subject to low sediment supply. *Water Resources Research*, *44*(12), W12202. https://doi.org/10.1029/2008wr007183

Singer, M. B. (2010). Transient response in longitudinal grain size to reduced gravel supply in a large river. *Geophysical Research Letters*, *37*(18). https://doi.org/10.1029/2010gl044381

Sklar, L. S., Riebe, C. S., Genetti, J., Leclere, S., & Lukens, C. E. (2020). Downvalley fining of hillslope sediment in an alpine catchment: Implications for downstream fining of sediment flux in mountain rivers. *Earth Surface Processes and Landforms*, *45*(8), 1828–1845. https://doi.org/10.1002/esp.4849

Sklar, L. S., Riebe, C. S., Marshall, J. A., Genetti, J., Leclere, S., Lukens, C. L., & Merces, V. (2017). The problem of predicting the size distribution of sediment supplied by hillslopes to rivers. *Geomorphology*, *277*, 31–49. https://doi.org/10.1016/j.geomorph.2016.05.005

Sternberg, H. (1875). Untersuchungen aber Lungen-und Querprofil geschiebefahrender Flasse. *Zeitschrift Far Bauwesen*, *25*, 483–506.

Sundborg, Å., & Sundborg, A. (1956). The river Klarälven a study of fluvial processes. *Geografiska Annaler*, *38*(2–3), 125–316. https://doi.org/10.2307/520285

Trampush, S. M., Huzurbazar, S., & McElroy, B. (2014). Empirical assessment of theory for bankfull characteristics of alluvial channels. *Water Resources Research*, *50*(12), 9211–9220. https://doi.org/10.1002/2014WR015597

Udden, J. A. (1914). Mechanical composition of clastic sediments. *GSA Bulletin*, *25*(1), 655–744. https://doi.org/10.1130/GSAB-25-655

Venditti, J. G., & Church, M. (2014). Morphology and controls on the position of a gravel-sand transition: Fraser River, British Columbia. *Journal of Geophysical Research: Earth Surface*, *119*(9), 1959–1976. https://doi.org/10.1002/2014JF003147

Venditti, J. G., Dietrich, W. E., Nelson, P. A., Wydzga, M. A., Fadde, J., & Sklar, L. (2010a). Effect of sediment pulse grain size on sediment transport rates and bed mobility in gravel bed rivers. *Journal of Geophysical Research*, *115*(F3), F03039. https://doi.org/10.1029/2009JF001418

Venditti, J. G., Dietrich, W. E., Nelson, P. A., Wydzga, M. A., Fadde, J., & Sklar, L. (2010b). Mobilization of coarse surface layers in gravel-bedded rivers by finer gravel bed load. *Water Resources Research*, *46*(7), W07506. https://doi.org/10.1029/2009WR008329

Venditti, J. G., Domarad, N., Church, M., & Rennie, C. D. (2015). The gravel-sand transition: Sediment dynamics in a diffuse extension. *Journal of Geophysical Research: Earth Surface*, *120*(6), 943–963. https://doi.org/10.1002/2014JF003328

Venditti, J. G., Nittrouer, J. A., Allison, M. A., Humphries, R. P., & Church, M. (2019). Supply-limited bedform patterns and scaling downstream of a gravel–sand transition. *Sedimentology*, *66*(6), 2538–2556. https://doi.org/10.1111/sed.12604

Wathen, S. J., Ferguson, R. I., Hoey, T. B., & Werritty, A. (1995). Unequal mobility of gravel and sand in weakly bimodal river sediments. *Water Resources Research*, *31*(8), 2087–2096. https://doi.org/10.1029/95WR01229

Wiberg, P. L., & Smith, J. D. (1987). Calculations of the critical shear stress for motion of uniform and heterogeneous sediments. *Water Resources Research*, *23*(8), 1471–1480. https://doi.org/10.1029/WR023i008p01471

Wilcock, P. R. (1998). Two-fraction model of initial sediment motion in gravel-bed rivers. *Science*, *280*(5362), 410–412. https://doi.org/10.1126/science.280.5362.410

Wilcock, P. R., & Crowe, J. C. (2003). Surface-based transport model for mixed-size sediment. *Journal of Hydraulic Engineering*, *129*(2), 120–128. https://doi.org/10.1061/(ASCE)0733-9429(2003)129:2(120)

Wilcock, P. R., & Kenworthy, S. T. (2002). A two-fraction model for the transport of sand/gravel mixtures. *Water Resources Research*, *38*(10), 12-1–12–12. https://doi.org/10.1029/2001WR000684

Wilcock, P. R., Kenworthy, S. T., & Crowe, J. C. (2001). Experimental study of the transport of mixed sand and gravel. *Water Resources Research*, *37*(12), 3349–3358. https://doi.org/10.1029/2001WR000683

Wilcock, P. R., & McArdell, B. W. (1993). Surface-based fractional transport rates: Mobilization thresholds and partial transport of a sand-gravel sediment. *Water Resources Research*, *29*(4), 1297–1312. https://doi.org/10.1029/92WR02748

Wilcock, P. R., & McArdell, B. W. (1997). Partial transport of a sand/gravel sediment. *Water Resources Research*, *33*(1), 235–245. https://doi.org/10.1029/96WR02672

Williams, G. P. (1970). *Flume width and water depth effects in sediment-transport experiments*. US Government Printing Office.

Wolcott, J. (1988). Nonfluvial control of bimodal grain-size distributions in river-bed gravels. *Journal of Sedimentary Research*, *58*(6), 979–984. https://doi.org/10.1306/212F8ED6-2B24-11D7-8648000102C1865D

Yalin, M. S., & Karahan, E. (1979). Inception of sediment transport. *Journal of the Hydraulics Division*, *105*(11), 1433–1443. https://doi.org/10.1061/JYCEAJ.0005306

Yatsu, E. (1955). On the longitudinal profile of the graded river. *Eos, Transactions American Geophysical Union*, *36*(4), 655–663. https://doi.org/10.1029/TR036i004p00655

Zimmermann, A., Church, M., & Hassan, M. A. (2010). Step-pool stability: Testing the jammed state hypothesis. *Journal of Geophysical Research*, *115*(F2), F02008. https://doi.org/10.1029/2009JF001365